

Phase Retrieval for Radar Waveform Design

Samuel Pinilla *Student Member, IEEE*, Kumar Vijay Mishra *Senior Member, IEEE*, Brian M. Sadler *Life Fellow, IEEE*, Henry Arguello *Senior Member, IEEE*

Abstract—The ability of a radar to discriminate in both range and Doppler velocity is completely characterized by the *ambiguity function* (AF) of its transmit waveform. Mathematically, it is obtained by correlating the waveform with its Doppler-shifted and delayed replicas. We consider the inverse problem of designing a radar transmit waveform that satisfies the specified AF magnitude. This process can be viewed as a signal reconstruction with some variation of phase retrieval methods. We provide a trust-region algorithm that minimizes a smoothed non-convex least-squares objective function to iteratively recover the underlying signal-of-interest for either time- or band-limited support. The method first approximates the signal using an iterative spectral algorithm and then refines the attained initialization based upon a sequence of gradient iterations. Our theoretical analysis shows that unique signal reconstruction is possible using signal samples no more than thrice the number of signal frequencies or time samples. Numerical experiments demonstrate that our method recovers both time- and band-limited signals from even sparsely and randomly sampled AFs with mean-square-error of 1×10^{-6} and 9×10^{-2} for the full noiseless samples and sparse noisy samples, respectively.

Index Terms—Ambiguity function, band-limited signals, non-convex optimization, phase retrieval, radar waveforms.

I. INTRODUCTION

THE mathematical theory of radar and sonar sensing widely employs cross-correlation technique for signal detection and parameter estimation. The transmit waveform correlated with its Doppler-shifted and delayed replicas yields *ambiguity function* (AF) that plays a key role in the detection and resolution theory of radar [1–3]. Through the AF, the transmit waveform enters into the performance analyses related to detection, target parameter accuracy, and resolution of multiple closely-spaced targets.

The AF was first introduced by Ville [4] and its significance as a signal design metric in the mathematical radar theory is credited to Woodward [5, 6], later expounded in detail by Siebert [7]. A radar system radiates a known waveform - characterized by its amplitude, frequency and polarization state - toward the targets-of-interest. When the radiated wave from the radar interacts with moving objects, all three characteristics of the scattered wave change. The detection and estimation of these changes helps in inferring the targets' size/shape, location relative to the radar, and radial Doppler velocity. Woodward observed that a suitable radar transmit signal should discriminate between the returning echoes from different targets and the AF should measure the uncertainty in such a discrimination.

S. P. and H. A. are with Universidad Industrial de Santander, Bucaramanga, Santander 680002 Colombia, e-mail: samuel.pinilla@correo.uis.edu.co, henarfu@uis.edu.co.

K. V. M. and B. S. are with the United States Army Research Laboratory, Adelphi, MD 20783 USA, e-mail: kvm@ieee.org, brian.m.sadler6.civ@army.mil.

This research was sponsored by the Army Research Office/Laboratory under Grant Number W911NF-21-1-0099, and the VIE project entitled “Dual blind deconvolution for joint radar-communications processing”. K. V. M. acknowledges support from the National Academies of Sciences, Engineering, and Medicine via Army Research Laboratory Harry Diamond Distinguished Postdoctoral Fellowship. S. P. acknowledges support from the EMET Research Institute in Colombia.

The conference precursor of this work was presented in the 2021 IEEE International Conference on Acoustics, Speech, and Signal Processing (ICASSP).

Woodward [5] defined a mean-squared error metric between a known waveform $x(t)$ and its replica with frequency-shift f and time-delay τ as

$$\Omega(\tau, f) = \int_{\mathbb{R}} |x(t) - x(t - \tau)e^{-i2\pi ft}|^2 dt.$$

In the expansion of this error metric, the only term that depends on the parameters is the inner product between the original waveform and its time-delayed/frequency-shifted version. The magnitude-squared inner product yields the narrow-band AF

$$A(\tau, f) = \left| \int_{\mathbb{R}} x(t)^* x(t - \tau) e^{-i2\pi ft} dt \right|^2. \quad (1)$$

The AF is not uniquely defined [8, 9], including in the works of Woodward [6]. Further, later works have generalized this definition to handle larger bandwidth signals [10, 11], long duration signals [12], volumetric scatterers [13, 14], targets with high velocity [15, 16], and angular domain [17–19]. The AF is also used in other applications such as optics [20–22]. Further, its relation to the uncertainty principle of quantum theory has also been implied [23]. In this paper, we restrict the discussion to the above-mentioned classical narrowband definition in the context of radar remote sensing.

The AF also plays a significant role in the detection theory of the targets because it represents the output of the matched filter at the receiver. It describes the interference caused by the range and/or Doppler of a target when compared to a reference target of equal radar cross-section. The ambiguity function evaluated at $(\tau, f) = (0, 0)$ is equal to the matched filter output that correlates perfectly to the signal reflected from the target of interest [24]. In other words, returns from the nominal target are located at the origin of the ambiguity function. Thus, the ambiguity function at nonzero τ and f represents returns from some range and Doppler different from those for the nominal target. Therefore, AF may be used to scale the signal-to-noise ratio (SNR) in detection analyses when the target and detector are mismatched [25].

The radar AF is used as an aid to select suitable radar waveforms. An AF equal to zero except at one point is ideal for detection tasks [26, Chapter 3]. But, in this case, the probability of the target lying within the response region would be near zero [27]. In the absence of an ideal AF, significant theoretical efforts have been devoted to the problem of finding functions of τ and f that are not only realizable as AFs but also have suitable radar performance. The resulting procedure of *waveform design* has traditionally focused on achieving AFs that are *thumbtack* with a sharp central spike and low sidelobes in the (τ, f) plane. Such an all-purpose AF is achieved by many conventional radar signals such as a narrowband pulse, linear frequency modulated (LFM) waveform, and stepped frequency pulse train [26]. Depending on the application, the AF may also be expressly shaped [28, 29]. For example, when the returning echo comprises multiple scatterers with varying strengths, the AFs of all targets are superimposed and shifted only by the relative differences in range and Doppler velocities. It is likely that the sidelobe of a stronger scatterer masks the main lobe of the weaker scatterer thereby hindering detection of the latter. In that case, the AF shaping is beneficial to avoid such masking in specific regions of the (τ, f) plane.

In this paper, we focus on the above-mentioned inverse problem of synthesizing waveforms that satisfy a given, desired, or specifically shaped ambiguity function. This has been studied extensively in the past, beginning with the least-squares approximations of Wilcox [30] and Sussman [31] over the entire τ - f plane to more recent formulations [32, 33] for specific regions in the τ - f plane. The AF of resulting waveform must satisfy the following properties [26, Chapter 3]:

P1 Assume the sampling periods in time and Doppler domains are Δt and Δf , respectively. The maximum value, say M , of the AF occurs at $(\Delta\tau, \Delta f) = (0, 0)$, i.e.,

$$\begin{aligned} \max\{A(\tau, f)\} &= A(0, 0) = M, \\ A(\tau, f) &\leq A(0, 0). \end{aligned} \quad (2)$$

P2 The total volume under the AF is the constant $\iint |A(\tau, f)|^2 d\tau df$.

P3 AF is symmetric in both τ and f , i.e., $A(\tau, f) = A(-\tau, -f)$.

P4 If the AF of $x(t)$ is $A(\tau, f)$, then the AF of $x(t) \exp(i\pi k t^2)$ is $A(\tau, f + k\tau)$.

For normalized signals ($M = 1$), it follows from **P1** on boundedness that the maximum value of $A(\tau, f)$ is unity at the origin. Further, **P2** states that the volume of $A(\tau, f)$ for normalized signals is also unity. Therefore, if $A(\tau, f)$ is squeezed to a narrow peak near to the origin, then that peak cannot exceed unity. The property **P3** indicates that the AF is symmetrical with respect to the origin. Finally, **P4** implies that multiplying the envelope of any signal by a quadratic phase (linear frequency) shears the shape of the AF. We refer the reader to [1] for the proofs of these properties.

The inverse waveform design problem exploits these properties to find a pulse that best fits the desired AF. For instance, [34] uses boundedness (**P1**) to show that when the AF is bounded by a *Hermite function*, i.e. a polynomial times the standard normal distribution with variance $\sigma^2 = 1/(2\pi)$, then the unknown signal is also a Hermite function where the polynomial is found from its AF by comparing the coefficients. The non-convex optimization employed in [33] employs the volume property (**P2**) to adaptively construct a Hermite function that best approximates the volume of a desired AF. More recent works such as [35–37] have proposed to numerically design the signal to improve the delay resolution of the AF in order to better determine the position of objects.

It follows from (1) that $A(\tau, f)$ is a phaseless mapping. In [34, 38], it was shown that **P1**–**P4** imply that the following *trivial ambiguities* or transformed versions of $x(t)$ lead to the same $A(\tau, f)$.

- T1** Rotated signal $e^{i\phi}x(t)$ for some $\phi \in \mathbb{R}$.
- T2** Translated signal $x(t - a)$ for some $a \in \mathbb{R}$.
- T3** Reflected signal $x(-t)$.
- T4** Scaled signal $e^{ibt}x(t)$ for some $b \in \mathbb{R}$.

Fig. 1 illustrates that different signals with such ambiguities map into the same AF. Finding radar waveforms that have only trivial partners is, therefore, equivalent to the phase retrieval (PR) problem [39] encountered in optics because $A(\tau, f)$ is a phaseless function [38]. In this work, we focus on PR approach to AF-based waveform design.

A. Prior art

The PR-based waveform design using a given AF is relatively unexamined when compared to AF-shaping optimization approaches [35]. The earliest instance is the seminal work of Rudolf De Buda [34] that showed recovery of Hermite functions from their (phaseless) AF. A few later works attempted to design code sequences with impulse-like correlations using the cyclic algorithm-new (CAN) and its variants (see [40] for a summary of this line of research). These

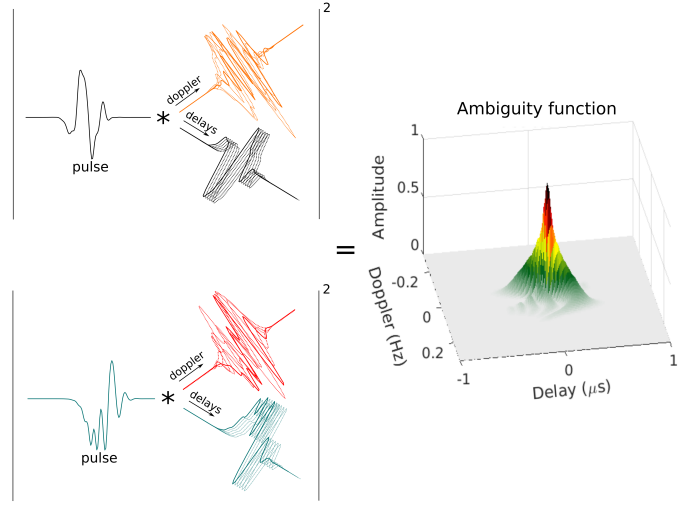


Fig. 1. Illustration of multiple signals with trivial ambiguities mapping to the same AF. On the left, two different signals on top and bottom are correlated with their Doppler- and delay-shifted replicas followed by the magnitude-squared operation.

methods are closely related to the classical least-squares recovery suggested by Sussman [31] and follow the alternating projection method detailed in the classical Gerchberg-Saxton PR algorithm (GSA) [41]. However, the convergence of GSA is usually to a local minimum and, therefore, its recovery abilities are limited (even in a noiseless setting). Moreover, the CAN-based waveform design in [40] does not produce a signal with specified AF but rather focuses on minimizing various sidelobe metrics (e.g., peak or integrated sidelobe levels) in the signal correlation.

More recently, [38, 42] applied the PR approach to the problem by exploiting the relationship between the AF and fractional Fourier transform (FrFT) [43] defined as

$$\mathcal{F}_{\alpha, \zeta}(x(t)) = c_{\alpha} e^{-i\pi|\zeta|^2 \cot(\alpha)} \int_{\mathbb{R}} x(t) e^{-i\pi t^2 \cot(\alpha)} e^{-\frac{i2\pi t \zeta}{\sin(\alpha)}} dt, \quad (3)$$

where $c_{\alpha} = \frac{e^{i/2(\alpha - \pi/2)}}{\sqrt{|\sin(\alpha)|}}$, $\alpha \in \mathbb{R} \setminus \pi\mathbb{Z}$ is the order (rotation angle) of the FrFT, and ζ models the FrFT frequency that is related to f by (1) as $f = \frac{\zeta}{\sin(\alpha)}$. Specifically, the Fourier magnitude of the product of the unknown signal with a conjugate time-shifted version of itself for several different shifts is equivalent to a frequency rotation using FrFT [38]. Mathematically, this equivalent definition is obtained for a time-shift $\tau = 0$ and frequency $\zeta = f \sin(\alpha)$ as

$$\begin{aligned} A_{\text{FrFT}}(\alpha, \zeta) &= \overbrace{\left| \int_{\mathbb{R}} \mathcal{F}_{\alpha, \zeta}(x(t)) \mathcal{F}_{\alpha, \zeta}^*(x(t)) e^{-i2\pi f t} dt \right|^2}^{A(0, \zeta) \text{ as in (1) for signal } \mathcal{F}_{\alpha}(x(t))} \\ &= \left| \int_{\mathbb{R}} \left| \int_{\mathbb{R}} x(t) e^{-i\pi t^2 \cot \alpha - \frac{i2\pi t \eta}{\sin \alpha}} dt \right|^2 e^{-i\zeta \eta} d\eta \right|^2. \end{aligned} \quad (4)$$

where A_{FrFT} represents the FrFT-based ambiguity function and η is the indexing Fourier frequency variable. When $\alpha = \pi/2$, (4) reduces to (1), i.e. $A_{\text{FrFT}}(\pi/2, \zeta) = A(0, f)$. It was shown in [38, 42] that Hermite function and rectangular pulse trains are uniquely identified from their respective FrFT-based AF. Extending the formulation in (4) to functions other than these two classes of signals is an open problem of high interest [32, 33]. Further, [17, 38, 42] do not provide a polynomial time computable procedure to estimate the signal from

TABLE I
COMPARISON WITH PRIOR ART

PR model	Measurements	Uniqueness Algorithm
STFT	$\mathbf{A}[p, k] := \left \sum_{n=0}^{N-1} \mathbf{x}[n] \mathbf{g}[pL - n] e^{-\frac{2\pi i k n}{N}} \right ^2, L < N$	Uniqueness (up to a global phase) for almost all signals for some L s and non-vanishing signal \mathbf{x} and window function \mathbf{g} [44]; Uniqueness if the first L samples of \mathbf{x} are known a priori for some L s and \mathbf{g} is non-vanishing [45]; Uniqueness (up to a global phase) for some L s, N s and mild conditions on \mathbf{g} [46] Non-convex algorithm [47] that employs an initialization followed by a gradient descent update rule.
FROG	$\mathbf{A}[p, k] := \left \sum_{n=0}^{N-1} \mathbf{x}[n] \mathbf{x}[pL + n] e^{-\frac{2\pi i k n}{N}} \right ^2, L < N$	Uniqueness (up to global phase, translated and reflected signal) for some L s and band-limited pulses [48]. Non-convex algorithm [49] that employs an initialization followed by a gradient descent update rule.
FrFT	$\mathbf{A}[\alpha, k] := \left \sum_{n=0}^{N-1} \left \sum_{t=0}^{N-1} \mathbf{x}[t] e^{\frac{-2i\pi t n - i\pi t^2 \cos(\alpha)}{\sin(\alpha)}} \right ^2 e^{-\frac{2i\pi n k}{N}} \right ^2$	Uniqueness (up to global phase, translated, reflected, and scaled signal) for Hermite and compact support functions, rectangular pulse trains and linear combinations of Gaussians [42]. No algorithm to solve this problem in polynomial time.
This paper	$\mathbf{A}[p, k] := \left \sum_{n=0}^{N-1} \mathbf{x}[n] \overline{\mathbf{x}[n-p]} e^{-\frac{2i\pi n k}{N}} \right ^2$	Uniqueness (up to global phase, translated, reflected and scaled signal) for band/time-limited signals. Non-convex algorithm that employs an initialization followed by a gradient descent update rule.

its AF. In this paper, we propose a non-convex PR algorithm that addresses these drawbacks.

Recall that PR constitutes an instance of non-convex programming, that is generally known to be NP-hard [50]. For instance, in case of real-valued signals, this would be a combinatorial optimization problem because it seeks a series of signs over the entries of the target signal that obey a given AF. For complex-valued signals, the procedure becomes more complicated and, instead of a set of signs, one must determine a collection of unimodular complex scalars that obey the given AF.

Substantial work has been done and is still ongoing to overcome the ill-posedness of the PR problem, and the literature is too large to summarize here (see, e.g., [51] for a contemporary survey, and references therein). Overall, two major approaches have emerged: the first harnesses prior knowledge of the signal structure, such as sparse support [52], non-vanishing behavior [47], or band-limitedness [53], while the other exploits technology to make additional measurements of the magnitude via, for example, coded diffraction patterns [39], masks [54], and short-time Fourier transform (STFT) [49]. These approaches employ traditional optimization strategies such as gradient descent [55] and semidefinite relaxations [39].

In particular, the AF-based signal recovery belongs to the class of one-dimensional (1-D) PR problems [56], wherein uniqueness of the retrieved signal cannot be ensured unless some conditions explained above are assumed for the signal. Note that a real 2-D signal is uniquely specified (up to the trivial ambiguities) by the magnitude of its continuous Fourier transform, with the exception of a set of signals of measure zero [56]. The 1-D AF-based signal design is bivariate in parameters τ and f . Among prior works, other similar bivariate 1-D problems include STFT [47] and frequency-resolve optical gating (FROG) [49] PR, apart from the previously mentioned FrFT formulation [42]. Table I summarizes and compares the discrete models, guarantees, and algorithms for various bivariate PR problems. Among these, the radar PR is the most challenging because of more trivial ambiguities than the other formulations.

B. Our contributions

In general, radar systems employ a wide variety of signals. Therefore, previous radar PR studies that were restricted to only

Hermite functions [34] or rectangular pulses [38] are not very useful in practice. In this paper, we extend AF-based waveform design to arbitrary signals that are time- or band-limited. We present a uniqueness result that states that band-limited (time-limited) signal can be recovered from its AF using at least $3B$ ($3S$) measurements, where B (S) is the signal's bandwidth (pulse-width). To this end, we develop a trust region algorithm that minimizes a smoothed non-convex least-squares objective function to iteratively estimate the band-limited signal of interest. The algorithm defines a region around the current iterate within which it trusts the model to be an adequate representation of the objective function. Then, it chooses the step to be an approximate minimizer of the model in this region. In particular, our proposed method consists of two steps: approximating the signal via an iterative spectral algorithm and subsequent refining of the attained initialization based upon a sequence of gradient iterations.

Our numerical experiments suggest that our proposed algorithm is able to estimate a band- or time-limited signal from its AF for both complete and incomplete measurements; here we consider the AF incomplete if only a few time-shifts or Fourier frequencies are considered in its formulation. Preliminary results of this work appeared in our conference publication [53], where we formulated AF-based waveform design of band-limited signals as a non-convex PR problem and solved it using *band-limited radar waveform design* via PR (BanRaW) algorithm. However, details of the uniqueness results, extension to time-limited signals, and extensive numerical experiments were excluded from [53]. In this paper, we include these details, present cases with incomplete/missing AF measurements and investigate additional practical constraints on signals such as linear/non-linear frequency modulated (LFM/NLFM) waveforms.

The rest of the paper is organized as follows. In the next section, we introduce the necessary background on the radar PR problem. In Section III, we develop our iterative procedure to refine the solution by minimizing a smooth least-squares objective. The spectral initialization step of this procedure is detailed in Section IV. We validate our models and methods through extensive numerical experiments in Section V. We conclude in Section VI.

Throughout this paper, we denote the sets of positive and strictly positive real numbers by $\mathbb{R}_+ := \{w \in \mathbb{R} : w \geq 0\}$ and $\mathbb{R}_{++} := \{w \in \mathbb{R} : w > 0\}$, respectively. We use boldface lowercase and

uppercase letters for vectors and matrices, respectively. The sets are denoted by calligraphic letters and $|\cdot|$ represents the cardinality of the set. The conjugate and conjugate transpose of the vector $\mathbf{w} \in \mathbb{C}^N$ are denoted as $\bar{\mathbf{w}} \in \mathbb{C}^N$ and $\mathbf{w}^H \in \mathbb{C}^N$, respectively. The n -th entry of a vector \mathbf{w} , which is assumed to be periodic, is written as $\mathbf{w}[n]$. We denote the Fourier transform of a vector and its conjugate reflected version (that is, $\hat{\mathbf{w}}[n] := \bar{\mathbf{w}}[-n]$) by $\tilde{\mathbf{w}}$ and $\hat{\mathbf{w}}$, respectively. The notation $\text{diag}(\mathbf{W}, \ell)$ refers to a column vector with entries $\mathbf{W}[j, (j + \ell) \bmod N]$ for $j = 0, \dots, N - 1$. For vectors, $\|\mathbf{w}\|_p$ is the ℓ_p norm. Additionally, we use \odot , and $*$ for the Hadamard (point-wise) product, and convolution, respectively; $\sqrt{\cdot}$ is the point-wise square root; superscript within parentheses as $(\cdot)^{(t)}$ indicates the value at t -th iteration; $\|\cdot\|_{\mathcal{F}}$ denotes the Frobenius norm of a matrix; $\text{Tr}(\cdot)$ denotes the matrix trace function; $\sigma_{\max}(\cdot)$ represents the largest singular value of its matrix argument; $\mathcal{R}(\cdot)$ denotes the real part of its complex argument; $\mathbb{E}[\cdot]$ represents the expected value; and $\omega = e^{\frac{2\pi i}{N}}$ is the N -th root of unity.

II. PROBLEM FORMULATION

The AF of a discrete signal $\mathbf{x} \in \mathbb{C}^N$ is a map $\mathbb{C}^N \rightarrow \mathbb{R}_+^{N \times N}$ defined as

$$\mathbf{A}[p, k] := \left| \sum_{n=0}^{N-1} \mathbf{x}[n] \overline{\mathbf{x}[n-p]} e^{-2i\pi n k / N} \right|^2. \quad (5)$$

This AF has symmetries or trivial ambiguities **T1-T4**, which naturally lead to the following measure of the relative error between the true signal \mathbf{x} and any $\mathbf{w} \in \mathbb{C}^N$. Here, the total number of AF measurements mb is the product of number of Doppler frequencies and time delays.

Definition 1. The distance between two vectors $\mathbf{x} \in \mathbb{C}^N$ and $\mathbf{w} \in \mathbb{C}^N$ is defined as

$$\text{dist}(\mathbf{x}, \mathbf{w}) := \frac{\|\sqrt{\mathbf{A}} - \sqrt{\mathbf{W}}\|_{\mathcal{F}}}{\|\sqrt{\mathbf{A}}\|_{\mathcal{F}}}, \quad (6)$$

where \mathbf{A} (\mathbf{W}) is the AF of \mathbf{x} (\mathbf{w}) according to (5). If $\text{dist}(\mathbf{x}, \mathbf{w}) = 0$ and the uniqueness conditions of Proposition 1 are met, then, for almost all signals, \mathbf{x} and \mathbf{z} are equal up to trivial ambiguities.

Our goal is to uniquely estimate the signal \mathbf{x} , up to trivial ambiguities, from the AF \mathbf{A} . To this end, we first show that such a recovery of \mathbf{x} is possible under rather mild conditions for a band-limited signal. We then extend this result to time-limited signals.

A. Uniqueness for band-limited signals

We introduce the following definition of a band-limited signal.

Definition 2 (B -band-limitedness). A signal $\mathbf{x} \in \mathbb{C}^N$ is defined to be B -band-limited if its Fourier transform $\tilde{\mathbf{x}} \in \mathbb{C}^N$ contains $N - B$ consecutive zeros. That is, there exists k such that $\tilde{\mathbf{x}}[k] = \dots = \tilde{\mathbf{x}}[N + k - B - 1] = 0$.

Recall two auxiliary lemmata. The following Lemma 1 states conditions to uniquely determine the signal \mathbf{x} from the knowledge of its power spectrum $|\tilde{\mathbf{x}}[k]|$.

Lemma 1. ([57, Corollary IV.3]) Denote the set of indices of unknown entries of signal \mathbf{x} by \mathcal{J} and $\mathcal{J} - \mathcal{J} = \{n_1 - n_2 | n_1, n_2 \in \mathcal{J}\}$ is the difference set. If $m \geq 2|\mathcal{J} - \mathcal{J}| - 1 + 2|\mathcal{J}|$ and $N > |\mathcal{J}|$ (that is, at least one signal entry is known), then almost every $\mathbf{x} \in \mathbb{C}^N$ is determined uniquely by $\{|\tilde{\mathbf{x}}[k]|\}_{k=0}^{m-1}$.

The conditions to uniquely determine the signal \mathbf{x} from the knowledge of its power spectrum $|\tilde{\mathbf{x}}[k]|$ and its absolute value $|\mathbf{x}[n]|$ are specified by the following Lemma 2.

Lemma 2. ([58, Corollary 2]) Almost every complex-valued signal $\mathbf{x} \in \mathbb{C}^N$ can be uniquely recovered from $\{|\tilde{\mathbf{x}}[k]|\}_{k=0}^{N-1}$ and $\{|\mathbf{x}[n]|\}_{n=0}^{N-1}$ up to rotations.

In Lemma 2, the phrase *almost every* or *almost all* means that the set of signals that cannot be uniquely determined, up to trivial ambiguities, is contained in the vanishing locus of a nonzero polynomial. In the following Proposition 1, we state the conditions for recovering band-limited signals from their AF.

Proposition 1. Assume $\mathbf{x} \in \mathbb{C}^N$ is a B -band-limited signal for some $B \leq N/2$. Then, almost all signals are uniquely determined from their AF $\mathbf{A}[p, k]$, up to trivial ambiguities, from $m \geq 3B$ measurements. If in addition we have access to the signal's power spectrum and $N \geq 3$, then $m \geq 2B$ measurements suffice.

Proof: We reformulate the measurement model to a more convenient structure. From the inverse Fourier transform, $\mathbf{x}[n] = \frac{1}{N} \sum_{k=0}^{N-1} \tilde{\mathbf{x}}[k] e^{2i\pi k n / N}$. The discrete form of inner product between the waveform and its time-delayed, frequency-shifted version is

$$\begin{aligned} \mathbf{S}[p, k] &= \sum_{n=0}^{N-1} \mathbf{x}[n] \overline{\mathbf{x}[n-p]} e^{-\frac{2i\pi n k}{N}} \\ &= \frac{1}{N^2} \sum_{n=0}^{N-1} \left(\sum_{\ell_1=0}^{N-1} \tilde{\mathbf{x}}[\ell_1] e^{\frac{2i\pi \ell_1 n}{N}} \right) \\ &\quad \times \left(\sum_{\ell_2=0}^{N-1} \tilde{\mathbf{x}}[\ell_2] e^{-\frac{2i\pi \ell_2 n}{N}} e^{\frac{2i\pi \ell_2 p}{N}} \right) e^{-\frac{2i\pi k n}{N}} \\ &= \frac{1}{N^2} \sum_{\ell_1, \ell_2=0}^{N-1} \tilde{\mathbf{x}}[\ell_1] \overline{\tilde{\mathbf{x}}[\ell_2]} e^{\frac{2i\pi \ell_2 p}{N}} \sum_{n=0}^{N-1} e^{\frac{2i\pi n (\ell_1 - \ell_2 - k)}{N}} \\ &= \frac{1}{N} \sum_{\ell=0}^{N-1} \tilde{\mathbf{x}}[\ell + k] \overline{\tilde{\mathbf{x}}[\ell]} e^{\frac{2i\pi \ell p}{N}}, \end{aligned} \quad (7)$$

where the last equality follows because the sum $\sum_{n=0}^{N-1} e^{\frac{2i\pi n (\ell_1 - \ell_2 - k)}{N}} = N$, if $\ell_1 = \ell_2 + k$ and zero otherwise. Obviously, $\mathbf{A}[p, k] = |\mathbf{S}[p, k]|^2$.

Assume that $B = N/2$, N is even, that $\tilde{\mathbf{x}}[n] \neq 0$ for $k = 0, \dots, B - 1$, and that $\tilde{\mathbf{x}}[n] = 0$ for $k = N/2, \dots, N - 1$. If the signal's nonzero Fourier coefficients are not in the interval $0, \dots, N/2 - 1$, then we can cyclically re-index the signal without affecting the proof. If N is odd, then we replace $N/2$ by $\lfloor N/2 \rfloor$ everywhere in the sequel. Clearly, the proof carries through for any $B \leq N/2$. From (7), the band-limitedness of the signal forms an "inverted pyramid" structure, in which each row represents fixed k and varying ℓ of $\tilde{\mathbf{x}}[\ell + k] \overline{\tilde{\mathbf{x}}[\ell]}$ for $k = 0, \dots, N/2 - 1$ as follows

$$\begin{aligned} &|\tilde{\mathbf{x}}[0]|^2, |\tilde{\mathbf{x}}[1]|^2, \dots, |\tilde{\mathbf{x}}[B-1]|^2, 0, \dots, 0 \\ &\overline{\tilde{\mathbf{x}}[0]} \tilde{\mathbf{x}}[1], \overline{\tilde{\mathbf{x}}[1]} \tilde{\mathbf{x}}[2], \dots, \overline{\tilde{\mathbf{x}}[B-2]} \tilde{\mathbf{x}}[B-1], 0, \dots, 0 \\ &\overline{\tilde{\mathbf{x}}[0]} \tilde{\mathbf{x}}[2], \overline{\tilde{\mathbf{x}}[1]} \tilde{\mathbf{x}}[3], \dots, \overline{\tilde{\mathbf{x}}[B-3]} \tilde{\mathbf{x}}[B-1], 0, \dots, 0 \\ &\vdots \\ &\overline{\tilde{\mathbf{x}}[0]} \tilde{\mathbf{x}}[B-1], 0, \dots, 0, 0, \dots, 0 \\ &0, 0, \dots, \overline{\tilde{\mathbf{x}}[0]} \tilde{\mathbf{x}}[B-1], 0, \dots, 0 \\ &0, \dots, \overline{\tilde{\mathbf{x}}[0]} \tilde{\mathbf{x}}[B-2], \overline{\tilde{\mathbf{x}}[1]} \tilde{\mathbf{x}}[B-1], 0, \dots, 0 \\ &\vdots \\ &0, \overline{\mathbf{x}}[0] \tilde{\mathbf{x}}[1], \overline{\tilde{\mathbf{x}}[1]} \tilde{\mathbf{x}}[2], \dots, \overline{\tilde{\mathbf{x}}[B-2]} \tilde{\mathbf{x}}[B-1], 0, \dots, 0. \end{aligned} \quad (8)$$

Then, it follows from (7) that $\mathbf{S}[p, k]$ is a subsample of the Fourier transform of each one of the pyramid's rows.

Step 0: From the $(B-1)$ -th row of (8),

$$|\mathbf{S}[p, B]| = |\tilde{\mathbf{x}}[0]| |\tilde{\mathbf{x}}[B-1]|, \forall p = 0, \dots, N-1. \quad (9)$$

The translation ambiguity **T2** is continuous. Therefore, we set $\tilde{\mathbf{x}}[0]$ to be real and, without loss of generality, assume $\tilde{\mathbf{x}}[0] = 1$ [53]. Then, from (9),

$$|\mathbf{S}[p, B-1]| = |\tilde{\mathbf{x}}[B-1]|, \forall p = 0, \dots, N-1. \quad (10)$$

Step 1: It follows from the first row of (8) that

$$|\mathbf{S}[p, 0]| = \frac{1}{N} \left| \sum_{\ell=0}^{B-1} |\tilde{\mathbf{x}}[\ell]|^2 e^{2\pi i \ell p/N} \right|, p = 0, \dots, N-1. \quad (11)$$

From **Step 0**, the entries $|\tilde{\mathbf{x}}[0]|$, $|\tilde{\mathbf{x}}[B-1]|$, and $\{|\mathbf{S}[p, 0]|\}_{p=0}^{N-1}$ are known. As per Lemma 1, for almost all signals we have that $|\tilde{\mathbf{x}}[1]|, \dots, |\tilde{\mathbf{x}}[B-2]|$ are uniquely determined. This does not imply that $\tilde{\mathbf{x}}[1], \dots, \tilde{\mathbf{x}}[B-1]$ are uniquely determined. In fact, there are up to 2^{B-1} vectors, modulo global phase, reflection and conjugation that satisfy the constraints in (9) and (11) [53].

Step 2: The second row of (8) yields the following system of equations

$$|\mathbf{S}[p, 1]| = \frac{1}{N} \left| \sum_{\ell=0}^{B-2} \tilde{\mathbf{x}}[\ell+1] \overline{\tilde{\mathbf{x}}[\ell]} e^{2\pi i \ell p/N} \right|, p = 0, \dots, N-1. \quad (12)$$

Fix one of the possible solutions for $\tilde{\mathbf{x}}[1]$ from **Step 1**. Since $\tilde{\mathbf{x}}[0]$ is known, it follows from Lemma 1 that for almost all signals $\tilde{\mathbf{x}}[1]\tilde{\mathbf{x}}[2], \dots, \tilde{\mathbf{x}}[B-1]\tilde{\mathbf{x}}[B-2]$ are uniquely determined.

Step 3: Now that $\tilde{\mathbf{x}}[0]$, and $\tilde{\mathbf{x}}[1]$ are known, $\tilde{\mathbf{x}}[2]$ can be estimated from **Step 2**. Thus, with known $\tilde{\mathbf{x}}[0]\tilde{\mathbf{x}}[2]$, Lemma 1 implies that for almost all signals $\tilde{\mathbf{x}}[1]\tilde{\mathbf{x}}[3], \dots, \tilde{\mathbf{x}}[B-3]\tilde{\mathbf{x}}[B-1]$ are uniquely determined. However, at this stage, there are still 2^{B-1} possible solutions from **Step 2**.

Despite a large number of possible solutions, we now prove that, at this step, there is only one out of the 2^{B-1} vectors in **Step 2** that is consistent with the constraints in (9), (11), and (12), up to trivial ambiguities. First, from **Step 1**, $|\tilde{\mathbf{x}}[0]|, \dots, |\tilde{\mathbf{x}}[B-1]|$ are uniquely determined. Therefore, from known $\{|\tilde{\mathbf{x}}[\ell]|\}_{\ell=0}^{B-1}$, and $\{|\mathbf{S}[p, 0]|\}_{p=0}^{N-1}$, Lemma 2 implies that $\tilde{\mathbf{x}}[1]\tilde{\mathbf{x}}[2], \dots, \tilde{\mathbf{x}}[B-1]\tilde{\mathbf{x}}[B-2]$ are uniquely determined for almost all signals. This now leads to a unique selection (up to trivial ambiguities) of $\tilde{\mathbf{x}}[1]$ in **Step 2**. Consequently, $\tilde{\mathbf{x}}[2]$ is uniquely determined in this step.

Step B-1: From previous B-2 steps, the entries $\tilde{\mathbf{x}}[0], \dots, \tilde{\mathbf{x}}[B-2]$ are uniquely determined (up to trivial ambiguities). Hence, it follows from Lemma 1 that $\tilde{\mathbf{x}}[B-1]$ is also uniquely determined.

At **Step 2** of the construction procedure described above, the signal $\tilde{\mathbf{x}}$ can be uniquely determined. This implies that $m \geq 3B$ measurements are required to solve the radar PR problem for band-limited signals. If, in addition, we have access to the spectrum $|\tilde{\mathbf{x}}|$, then we can uniquely determined $\tilde{\mathbf{x}}$ at **Step 1** if $N \geq 3$. Therefore, under this scenario, only $m \geq 2B$ measurements are needed. ■

Note that Proposition 1 states that all delay steps are not needed to recover the signal. Therefore, it is desired to develop a method that also works for such partial measurements. Step 5 of the proof reveals that the first and the $(B-1)$ -th rows of AF in (5) must be perfectly preserved in order to ensure uniqueness (up to trivial ambiguities).

B. Uniqueness for time-limited signals

We analogously specify the time-limited signals via the Definition 3 as follows.

Definition 3 (*S*-time-limitedness). A signal $\mathbf{x} \in \mathbb{C}^N$ is defined to be *S*-time-limited signal if it contains $N-S$ consecutive zeros. That is, there exists k such that $\mathbf{x}[k] = \dots = \mathbf{x}[N+k-S-1] = 0$.

Then, following Proposition 1, the corresponding result for time-limited waveforms is stated by the Corollary 1 below. The notion of *almost all* signals here is the same as in Proposition 1.

Corollary 1. Assume $\mathbf{x} \in \mathbb{C}^N$ is a *S*-band-limited signal for some $S \leq N/2$. Then, almost all signals are uniquely determined from their AF $\mathbf{A}[p, k]$, up to trivial ambiguities, from $m \geq 3S$ measurements. If in addition we have access to the signal's power and $N \geq 3$, then $m \geq 2S$ measurements suffice.

Proof: Recall that, according to (5), we have

$$\mathbf{A}[p, k] = \left| \sum_{n=0}^{N-1} \mathbf{x}[n] \overline{\mathbf{x}[n-p]} e^{-2i\pi nk/N} \right|^2. \quad (13)$$

Assume that $S = N/2$, N is even, that $\mathbf{x}[n] \neq 0$ for $n = 0, \dots, S-1$, and that $\mathbf{x}[n] = 0$ for $n = N/2, \dots, N-1$. If the signal's nonzero coefficients are not in the interval $0, \dots, N/2-1$, then we can cyclically reindex the signal without affecting the proof. If N is odd, then one should replace $N/2$ by $\lfloor N/2 \rfloor$ everywhere in the sequel. Clearly, the proof carries through for any $S \leq N/2$.

It follows from (7) that the bandlimitedness of the signal forms a "inverted pyramid" structure. Here, each row represents fixed p and varying n of $\mathbf{x}[n-p]\mathbf{x}[n]$ for $p = 0, \dots, N/2-1$ as follows

$$\begin{aligned} & |\mathbf{x}[0]|^2, |\mathbf{x}[1]|^2, \dots, |\mathbf{x}[S-1]|^2, 0, \dots, 0 \\ & 0, \overline{\mathbf{x}[0]}\mathbf{x}[1], \overline{\mathbf{x}[1]}\mathbf{x}[2], \dots, \overline{\mathbf{x}[S-2]}\mathbf{x}[S-1], 0, \dots, 0 \\ & 0, 0, \overline{\mathbf{x}[0]}\mathbf{x}[2], \overline{\mathbf{x}[1]}\mathbf{x}[3], \dots, \overline{\mathbf{x}[S-3]}\mathbf{x}[S-1], 0, \dots, 0 \\ & \vdots \\ & 0, 0, \dots, 0, \overline{\mathbf{x}[0]}\mathbf{x}[S-1], 0, \dots, 0, 0, \dots, 0 \\ & \mathbf{x}[0]\overline{\mathbf{x}[S-1]}, 0, 0, \dots, 0 \\ & \mathbf{x}[0]\overline{\mathbf{x}[S-2]}, \mathbf{x}[1]\overline{\mathbf{x}[S-1]}, 0, 0, \dots, 0 \\ & \vdots \\ & \mathbf{x}[0]\overline{\mathbf{x}[1]}, \mathbf{x}[1]\overline{\mathbf{x}[2]}, \dots, \mathbf{x}[S-2]\overline{\mathbf{x}[S-1]}, 0, 0, \dots, 0. \end{aligned} \quad (14)$$

Then, $\mathbf{A}[p, k]$ as in (13) is a subsample of the Fourier transform of each one of the pyramid's rows.

Therefore, performing an analogous construction procedure as in Proposition 1 on (14), we have that the signal \mathbf{x} can be uniquely determined from $m \geq 3S$ measurements. If the power $|\mathbf{x}|$ of the signal is additionally available, we can uniquely determine \mathbf{x} for $N \geq 3$. This implies that under this scenario only $m \geq 2S$ measurements are needed. ■

The proof of Corollary 1 is also a construction procedure as in the proof of Proposition 1, and that the first and the $(S-1)$ -th rows of the AF in (5) must be perfectly preserved in order to ensure uniqueness (up to trivial ambiguities).

C. AF-based PR optimization

It is instructive to note that the the AF-based PR requires recovering a signal from phaseless quadratic random measurements. Among prior works on similar problems, a popular approach is to minimize the intensity least-squares objective [55]. A few recent works have further shown that this technique leads to better reconstruction under noisy scenarios [59]. However, the amplitude least-squares cost function is non-smooth and thus may lead to a biased descent direction [60]. In [59], the non-smoothness was addressed by

introducing truncation parameters into the gradient step in order to eliminate the errors in the estimated descent direction. However, this procedure may modify the search direction and increase the sample complexity of the PR problem [60]. The smoothing strategy recently proposed in [60] overcomes these shortcomings.

Following [60], define a function $\varphi_\mu : \mathbb{R} \rightarrow \mathbb{R}_{++}$ as

$$\varphi_\mu(w) := \sqrt{w^2 + \mu^2},$$

where $\mu \in \mathbb{R}_{++}$ is a tunable parameter. The first stage of our algorithm is to recover the underlying signal \mathbf{z} by considering the smooth version of amplitude least-squares objective as follows

$$\underset{\mathbf{z} \in \mathbb{C}^N}{\text{minimize}} h(\mathbf{z}, \mu) = \underset{\mathbf{z} \in \mathbb{C}^N}{\text{minimize}} \frac{1}{N^2} \sum_{k,p=0}^{N-1} \ell_{k,p}(\mathbf{z}, \mu), \quad (15)$$

where

$$\ell_{k,p}(\mathbf{z}, \mu) := \left[\varphi_\mu \left(\left| \sum_{n=0}^{N-1} \mathbf{z}[n] \overline{\mathbf{z}[n-p]} e^{-2\pi i n k / N} \right| \right) - \sqrt{\mathbf{A}[p, k]} \right]^2. \quad (16)$$

Note that when $\mu = 0$, (16) reduces to a non-smooth formulation.

III. RECONSTRUCTION ALGORITHM

To solve (15), we now propose a trust region algorithm based on the Cauchy point, which lies on the gradient and minimises the quadratic cost function by iteratively refining the trust region of the solution. We suggest minimizing the objective in (15) by employing a Cauchy point update rule, namely, by iteratively applying

$$\mathbf{x}^{(t+1)} := \mathbf{x}^{(t)} + \alpha^{(t)} \mathbf{b}^{(t)}, \quad (17)$$

where $\alpha^{(t)}$ is the step size at iteration t and gradient descent direction vector is

$$\begin{aligned} \mathbf{b}^{(t)} &:= \arg \min_{\mathbf{b} \in \mathbb{C}^n} h(\mathbf{x}^{(t)}, \mu^{(t)}) + 2\mathcal{R}(\mathbf{b}^H \mathbf{d}^{(t)}) \\ &\text{subject to} \quad \|\mathbf{b}\|_2 \leq \mu^{(t)}, \end{aligned} \quad (18)$$

where $\mathbf{d}^{(t)}$ is the gradient of $h(\mathbf{z}, \mu)$ with respect to $\bar{\mathbf{z}}$ at iteration t . The solution to (18) is [61, Chapter 4]

$$\mathbf{b}^{(t)} = -\frac{\mu^{(t)}}{\|\mathbf{d}^{(t)}\|_2} \mathbf{d}^{(t)}. \quad (19)$$

To directly compute the gradient $\mathbf{d}^{(t)}$, we employ Wirtinger derivatives [62], which are partial first-order derivatives of complex variables with respect to a real variable. Define

$$\mathbf{f}_k^H := [\omega^{-0(k-1)}, \omega^{-1(k-1)}, \dots, \omega^{-(N-1)(k-1)}]. \quad (20)$$

The Wirtinger derivative of $h(\mathbf{z}, \mu)$ in (15) with respect to $\bar{\mathbf{z}}[\ell]$ is

$$\begin{aligned} \frac{\partial h(\mathbf{z}, \mu)}{\partial \bar{\mathbf{z}}[\ell]} &:= \frac{1}{N^2} \sum_{k,p=0}^{N-1} \left(\mathbf{f}_k^H \mathbf{g}_p - v_{k,p} \right) \mathbf{z}[\ell - p] e^{2\pi i \ell k / N} \\ &\quad + \frac{1}{N^2} \sum_{k,p=0}^{N-1} \left(\mathbf{f}_k^T \overline{\mathbf{g}_p} - v_{k,p} \right) \mathbf{z}[\ell + p] e^{-2\pi i (\ell + p) k / N}, \end{aligned} \quad (21)$$

where $v_{k,p} := \frac{\sqrt{\mathbf{A}[p, k]}}{\varphi_\mu(\|\mathbf{f}_k^H \mathbf{g}_p\|)} \frac{\mathbf{f}_k^H \mathbf{g}_p}{\varphi_\mu(\|\mathbf{f}_k^H \mathbf{g}_p\|)}$ and $\mathbf{g}_p := [\mathbf{z}[0] \overline{\mathbf{z}[p]}, \dots, \mathbf{z}[N-1] \overline{\mathbf{z}[N-1+p]}]^T$. The gradient $\mathbf{d}^{(t)}$ becomes

$$\mathbf{d}^{(t)} := \left[\frac{\partial h(\mathbf{x}^{(t)}, \mu)}{\partial \bar{\mathbf{z}}[0]}, \dots, \frac{\partial h(\mathbf{x}^{(t)}, \mu)}{\partial \bar{\mathbf{z}}[N-1]} \right]^T. \quad (22)$$

The sum in (21) depends on the size N of the vector \mathbf{z} and, therefore, the computational time to compute (21) scales linearly with N . To address the computational complexity and memory requirements for large N , we adopt a block stochastic gradient descent strategy. That is, instead of calculating (21), we choose only a random subset of the sum for each iteration t . Define a set $\Gamma_{(t)}$ chosen uniformly and independently at random at each iteration t from subsets of $\{1, \dots, N\}^2$ with cardinality $Q \in \{1, \dots, N^2\}$. Then, the new gradient vector is

$$\begin{aligned} \mathbf{d}_{\Gamma_{(t)}}[\ell] &= \sum_{p,k \in \Gamma_{(t)}} \left(\mathbf{f}_k^H \mathbf{g}_p^{(t)} - v_{k,p,t} \right) \mathbf{x}^{(t)}[\ell - p] e^{2\pi i \ell k / N} \\ &\quad + \sum_{p,k \in \Gamma_{(t)}} \left(\mathbf{f}_k^T \overline{\mathbf{g}_p}^{(t)} - v_{k,p} \right) \mathbf{x}^{(t)}[\ell + p] e^{-2\pi i (\ell + p) k / N}. \end{aligned} \quad (23)$$

Specifically, we achieve this by uniformly sampling the gradient in (22) using a minibatch data of size Q for each update step, such that the expectation $\mathbb{E}_{\Gamma_{(t)}}[\mathbf{d}_{\Gamma_{(t)}}]$ is (21) [63, page 130]. Our algorithm is summarized in Algorithm 1 below.

Algorithm 1 Estimating band/time-limited signal from AF-based PR

Input: Data $\{\mathbf{A}[p, k] : k, p = 0, \dots, N-1\}$, constants $\gamma_1, \gamma, \alpha \in (0, 1)$, $\mu^{(0)} \geq 0$, cardinality $Q \in \{1, \dots, N^2\}$, tolerance $\epsilon > 0$, and number of iterations T .

Output: Estimate $\mathbf{x}^{(T)}$ of \mathbf{x} .

- 1: Initial point $\mathbf{x}^{(0)}$ (from Algorithm 2).
 - 2: **while** $\|\mathbf{b}_{\Gamma_{(t)}}\|_2 \geq \epsilon$ or $t \leq T$ **do**
 - 3: Choose $\Gamma_{(t)}$ uniformly at random from the subsets of $\{1, \dots, N\}^2$ with cardinality Q .
 - 4: $\mathbf{x}^{(t+1)} \leftarrow \mathbf{x}^{(t)} + \alpha^{(t)} \mathbf{b}_{\Gamma_{(t)}} = \mathbf{x}^{(t)} - \alpha^{(t)} \frac{\mu^{(t)}}{\|\mathbf{d}_{\Gamma_{(t)}}\|_2} \mathbf{d}_{\Gamma_{(t)}}$,
where
 - 5: $v_{k,p,t} \leftarrow \sqrt{\mathbf{A}[p, k]} \frac{\mathbf{f}_k^H \mathbf{g}_p^{(t)}}{\varphi_{\mu^{(t)}}(\|\mathbf{f}_k^H \mathbf{g}_p^{(t)}\|)}$.
 - 6: $\mathbf{g}_p^{(t)} \leftarrow [\mathbf{x}^{(t)}[0] \overline{\mathbf{x}^{(t)}[p]}, \dots, \mathbf{x}^{(t)}[N-1] \overline{\mathbf{x}^{(t)}[N-1+p]}]^T$.
 - 7: **if** $\|\mathbf{d}_{\Gamma_{(t)}}\|_2 \geq \gamma \mu^{(t)}$ **then** $\mu^{(t+1)} = \mu^{(t)}$.
 - 8: **else** $\mu^{(t+1)} = \gamma_1 \mu^{(t)}$.
 - 9: **return:** $\mathbf{x}^{(T)}$.
-

As mentioned in Section II-C, choosing $\mu > 0$ leads to a smooth cost function. This prevents a bias in the update direction and we are able to construct a descent rule for μ (line 13 of Algorithm 1) in order to guarantee convergence to a first-order optimal point (that is, a point with zero gradient) in the vicinity of the solution. Note that we initialize the algorithm through a minimally iterative spectral procedure described in the next section. The following Theorem 1 states the convergence conditions of Algorithm 1.

Theorem 1. Let \mathbf{x} be S -time-limited or B -band-limited for some $S \leq N/2$ or $B \leq N/2$, respectively, satisfying $\text{dist}(\mathbf{x}, \mathbf{x}^{(t)}) \leq \rho$ for some sufficiently small constant $\rho > 0$. Suppose that $\Gamma_{(t)}$ is sampled uniformly at random from all subsets of $\{1, \dots, N\}^2$ with cardinality Q , independently for each iteration. Then, for almost all

signals, Algorithm 1 with step size $\alpha \in (0, \frac{2}{U}]$ satisfies

$$\lim_{t \rightarrow \infty} \mu^{(t)} = 0, \text{ and } \lim_{t \rightarrow \infty} \|\mathbf{d}^{(t)}\|_2 = 0, \quad (24)$$

for some constant $U > 0$ depending on ρ .

Proof: See Appendix A. ■

The result in Theorem 1 in guaranteeing convergence of Algorithm 1 is significant because prior works lack polynomial time algorithms to solve the AF-based PR. Note that the presence of conjugate term in the AF measurements complicates this problem with additional trivial ambiguities when compared to other bivariate PR problems such as FROG [49] and STFT [44]. The key to the proof of Theorem 1 is the update rule for the smoothing value $\mu^{(t)}$ in lines 7-8 in Algorithm 1. This rule controls the magnitude of the gradient descent direction vector $\mathbf{d}_{\Gamma(t)}$ leading to its minimization with the iterative decrease in $\mu^{(t)}$.

IV. INITIALIZATION ALGORITHM

The unconstrained minimization of the function in (15) is a non-convex problem for which there is no guarantee that an arbitrary initialization will converge to a global minimum. We therefore devise a method to initialize the gradient iterations. This strategy approximates the signal \mathbf{x} from the AF as the leading eigenvector (with appropriate normalization) of a carefully designed matrix that approximates the correlation matrix of the signal \mathbf{x} .

Instead of directly dealing with the AF in (5), we consider the acquired data in a transformed domain by taking its 1-D discrete Fourier transform (DFT) with respect to the frequency variable (normalized by $1/N$). Our measurement model is then

$$\begin{aligned} \mathbf{Y}[p, \ell] &= \frac{1}{N} \sum_{k=0}^{N-1} \mathbf{A}[p, k] e^{-2\pi i k \ell / N} \\ &= \frac{1}{N} \sum_{k, n, m=0}^{N-1} \mathbf{x}[n] \overline{\mathbf{x}[n-p]} \mathbf{x}[m-p] \overline{\mathbf{x}[m]} e^{-2\pi i k \frac{(m-n-\ell)}{N}} \\ &= \sum_{n=0}^{N-1} \mathbf{x}[n] \overline{\mathbf{x}[n-p]} \mathbf{x}[n+\ell-p] \overline{\mathbf{x}[n+\ell]}, \end{aligned} \quad (25)$$

where $p, \ell = 0, \dots, N-1$. Observe that, for fixed p , $\mathbf{Y}[p, \ell]$ is the autocorrelation of $\mathbf{x} \odot \overline{\mathbf{x}}_p$, where $\mathbf{x}_p[n] = \mathbf{x}[n-p]$.

Define $\mathbf{D}_p \in \mathbb{C}^{N \times N}$ be a diagonal matrix composed of the entries of \mathbf{x}_p , and let \mathbf{C}_ℓ be a circulant matrix that shifts the entries of a vector by ℓ locations, namely, $(\mathbf{C}_\ell \mathbf{x})[n] = \mathbf{x}[n+\ell]$. Then, the matrix $\mathbf{X} := \mathbf{x} \mathbf{x}^H$ is linearly mapped to $\mathbf{Y}[p, \ell]$ as follows:

$$\begin{aligned} \mathbf{Y}[p, \ell] &= (\overline{\mathbf{D}}_{p+\ell} \mathbf{D}_p \mathbf{C}_\ell \mathbf{x})^H \mathbf{x} = \mathbf{x}^H \mathbf{A}_{p, \ell} \mathbf{x} \\ &= \text{Tr}(\mathbf{X} \mathbf{A}_{p, \ell}), \end{aligned} \quad (26)$$

where $\mathbf{A}_{p, \ell} = \mathbf{C}_{-\ell} \overline{\mathbf{D}}_p \mathbf{D}_{p+\ell}$. Observe that $\mathbf{C}_\ell^T = \mathbf{C}_{-\ell}$. Thus,

$$\mathbf{y}_\ell = \mathbf{G}_\ell \mathbf{x}_\ell, \quad (27)$$

for a fixed $\ell \in \{0, \dots, N-1\}$, where $\mathbf{y}_\ell[n] = \mathbf{Y}[n, \ell]$ and $\mathbf{x}_\ell = \text{diag}(\mathbf{X}, \ell)$. The (p, n) -th entry of the matrix $\mathbf{G}_\ell \in \mathbb{C}^{\lceil \frac{N}{L} \rceil \times N}$ is

$$\mathbf{G}_\ell[p, n] := \overline{\mathbf{x}_p[n]} \mathbf{x}_p[n+\ell]. \quad (28)$$

From (28) it follows that \mathbf{G}_ℓ is a circulant matrix. Therefore, \mathbf{G}_ℓ is invertible if and only if the DFT of its first column, i.e. $\overline{\mathbf{x}} \odot (\mathbf{C}_\ell \mathbf{x})$, is non-vanishing.

Using (27), we propose a method to estimate the signal \mathbf{x} from measurements (5) using an alternating method: fix \mathbf{G}_ℓ , solve for \mathbf{x}_ℓ , update \mathbf{G}_ℓ and so forth. After a few iterations of this two-step procedure, the output is used to initialize the gradient Algorithm 1.

This alternating scheme is summarized in Algorithm 2. We begin with the initial point

$$\mathbf{x}_{\text{init}}[p] := \mathbf{v}[p] \exp(i\theta[p]), \quad (29)$$

where $\theta[r] \in [0, 2\pi)$ is chosen uniformly at random for all $r \in \{0, \dots, N-1\}$. The r -th entry of \mathbf{v} corresponds to the summation of the measured AF over the frequency axis:

$$\begin{aligned} \mathbf{v}[p] &:= \frac{1}{N} \sum_{k=0}^{N-1} \mathbf{A}[p, k] = \sum_{k=0}^{N-1} \left| \sum_{n=0}^{N-1} \mathbf{x}[n] \overline{\mathbf{x}[n-p]} e^{-2\pi i n k / N} \right|^2 \\ &:= \sum_{n=0}^{N-1} |\mathbf{x}[n]|^2 |\mathbf{x}[n-p]|^2. \end{aligned} \quad (30)$$

Once \mathbf{x}_{init} is constructed, the vectors $\mathbf{x}_\ell^{(t)}$ at $t=0$ are constructed as

$$\mathbf{x}_\ell^{(0)} = \text{diag}(\mathbf{X}_0^{(0)}, \ell), \quad (31)$$

where

$$\mathbf{X}_0^{(0)} = \mathbf{x}_{\text{init}} \mathbf{x}_{\text{init}}^H. \quad (32)$$

Then, from (31), we proceed with an alternating procedure between estimating the matrix \mathbf{G}_ℓ , and updating the vector \mathbf{x}_ℓ as follows.

- *Update rule for \mathbf{G}_ℓ :* In order to update \mathbf{G}_ℓ , we update the matrix $\mathbf{X}_0^{(t)}$ as

$$\text{diag}(\mathbf{X}_0^{(t)}, \ell) = \mathbf{x}_\ell^{(t)}. \quad (33)$$

Observe that if $\mathbf{x}_\ell^{(t)}$ is close to \mathbf{x}_ℓ for all ℓ , then $\mathbf{X}_0^{(t)}$ is close to $\mathbf{x} \mathbf{x}^H$. Assume $\mathbf{w}^{(t)}$ to be the leading (unit-norm) eigenvector of the matrix $\mathbf{X}_0^{(t)}$ constructed in (33). From (28), each matrix $\mathbf{G}_\ell^{(t)}$ at iteration t is

$$\mathbf{G}_\ell^{(t)}[p, n] = \overline{\mathbf{x}_p^{(t)}}[n] \mathbf{x}_p^{(t)}[n+\ell], \quad (34)$$

where $\mathbf{x}_p^{(t)}[n] = \mathbf{w}^{(t)}[n-p]$.

- *Optimization with respect to \mathbf{x}_ℓ :* For a fixed $\mathbf{G}_\ell^{(t-1)}$, we estimate $\mathbf{x}_\ell^{(t)}$ at iteration t by solving the linear least-squares (LS) problem

$$\underset{\mathbf{p}_\ell \in \mathbb{C}^N}{\text{minimize}} \quad \|\mathbf{y}_\ell - \mathbf{G}_\ell^{(t-1)} \mathbf{p}_\ell\|_2^2. \quad (35)$$

The relationship between the vectors $\mathbf{x}_\ell^{(t)}$ is ignored at this stage. If $\mathbf{G}_\ell^{(t-1)}$ is invertible, then the solution to this problem is given by $(\mathbf{G}_\ell^{(t-1)})^{-1} \mathbf{y}_\ell$. Since $\mathbf{G}_\ell^{(t-1)}$ is a circulant matrix, it is invertible if and only if the DFT of $\overline{\mathbf{x}}^{(t-1)} \odot (\mathbf{C}_\ell \mathbf{x}^{(t-1)})$ is non-vanishing. In general, this condition cannot be ensured. Thus, we propose a surrogate proximal optimization problem to estimate $\mathbf{x}_\ell^{(t)}$ by

$$\underset{\mathbf{p}_\ell \in \mathbb{C}^N}{\text{minimize}} \quad \|\mathbf{y}_\ell - \mathbf{G}_\ell^{(t-1)} \mathbf{p}_\ell\|_2^2 + \frac{1}{2\lambda_{(t)}} \|\mathbf{p}_\ell - \mathbf{x}_\ell^{(t-1)}\|_2^2, \quad (36)$$

where $\lambda_{(t)} > 0$ is a regularization parameter. In practice, $\lambda_{(t)}$ is a tunable parameter [64]. Specifically, in this work, the value of $\lambda_{(t)}$ was determined using a cross-validation strategy such that each simulation uses the value that results in the smallest relative error according to (6). The surrogate optimization problem in (36) is strongly convex [64], and admits the following closed form solution

$$\mathbf{x}_\ell^{(t)} = \mathbf{B}_{\ell, t}^{-1} \mathbf{e}_{\ell, t}, \quad (37)$$

where

$$\begin{aligned} \mathbf{B}_{\ell, t} &= \left(\mathbf{G}_\ell^{(t-1)} \right)^H \left(\mathbf{G}_\ell^{(t-1)} \right) + \frac{1}{2\lambda} \mathbf{I}, \\ \mathbf{e}_{\ell, t} &= \left(\mathbf{G}_\ell^{(t)} \right)^H \mathbf{y}_\ell + \frac{1}{2\lambda} \mathbf{x}_\ell^{(t-1)}, \end{aligned} \quad (38)$$

Algorithm 2 Initialization of AF-based PR

Input: Measurements $\mathbf{A}[p, k]$, number of iterations T , and $\lambda > 0$.
Output: Estimate $\mathbf{x}^{(0)}$ of \mathbf{x} .

- 1: **Initialize:** $\mathbf{x}_{\text{init}}[p] \leftarrow \mathbf{v}[p] \exp(i\theta[p])$, and $\mathbf{v}[p] \leftarrow \frac{1}{N} \sum_{k=0}^{N-1} \mathbf{A}[p, k]$,
 $\theta[p] \in [0, 2\pi]$ is chosen uniformly and independently at random.
- 2: Compute $\mathbf{Y}[p, \ell]$ the 1-D inverse DFT with respect to k of $\mathbf{A}[p, k]$.
- 3: **for** $t = 1$ to T **do**
- 4: Construct $\mathbf{G}_\ell^{(t)}$ according to (34).
- 5: $\mathbf{B}_{\ell, t} \leftarrow (\mathbf{G}_\ell^{(t)})^H (\mathbf{G}_\ell^{(t)}) + \frac{1}{2\lambda} \mathbf{I}$.
- 6: $\mathbf{e}_{\ell, t} \leftarrow (\mathbf{G}_\ell^{(t)})^H \mathbf{y}_\ell + \frac{1}{2\lambda} \mathbf{x}_\ell^{(t-1)}$.
- 7: Construct the matrix $\mathbf{X}_0^{(t)}$ such that $\text{diag}(\mathbf{X}_0^{(t)}, \ell) = \mathbf{B}_{\ell, t}^{-1} \mathbf{e}_{\ell, t}$, $\ell = 0, \dots, N-1$.
- 8: Set $\mathbf{w}^{(t)}$ be the leading (unit-norm) eigenvector of $\mathbf{X}_0^{(t)}$.
- 9: $\mathbf{x}_p^{(t)}[n] \leftarrow \mathbf{w}^{(t)}[n - p]$.
- 10: $\mathbf{x}^{(0)} \leftarrow \sqrt[4]{\sum_{n \in \mathcal{S}} (\mathbf{B}_{0, T}^{-1} \mathbf{e}_{0, T})[n] \mathbf{w}^{(T)}[n]}$, where $\mathcal{S} := \{n : (\mathbf{B}_{0, T}^{-1} \mathbf{e}_{0, T})[n] > 0\}$.
- 11: **return:** $\mathbf{x}^{(0)}$.

with $\mathbf{I} \in \mathbb{R}^{N \times N}$ the identity matrix. Clearly $\mathbf{B}_{\ell, t}$ in (38) is always invertible. The update step for each $\mathbf{x}_\ell^{(t)}$ is computed in line 9 of Algorithm 2.

Finally, in order to estimate \mathbf{x} , the (unit-norm) principal eigenvector of $\mathbf{X}_0^{(T)}$ is normalized by

$$\beta = \sqrt[4]{\sum_{n \in \mathcal{S}} (\mathbf{B}_{0, T}^{-1} \mathbf{e}_{0, T})[n]}, \quad (39)$$

where $\mathcal{S} := \{n : (\mathbf{B}_{0, T}^{-1} \mathbf{e}_{0, T})[n] > 0\}$ is the set with indices that correspond to the positive entries of the vector $\mathbf{B}_{0, T}^{-1} \mathbf{e}_{0, T}$. Observe that (39) results from the fact that $\sum_{n=0}^{N-1} \text{diag}(\mathbf{X}, 0)[n] = \|\mathbf{x}\|_2^4$.

The following Theorem 2 establishes that the resulting $\mathbf{x}^{(0)}$ from the update rules in (34) and (37) leads to a close estimation of the real unknown signal \mathbf{x} for complete radar AF.

Theorem 2. Assume that \mathbf{A} in (5) is complete and the regularization parameter $\lambda_{(t)}$ satisfies $\lambda_{(t)} \sigma_{\min}^2(\mathbf{G}^{(t-1)}) > 1/2$ for all $t > 0$. Then, initializing with \mathbf{x}_{init} in (29), the estimated vector $\mathbf{x}^{(0)}$ in Algorithm 2 satisfies

$$\|\mathbf{x}^{(0)}(\mathbf{x}^{(0)})^H - \mathbf{x}\mathbf{x}^H\|_{\mathcal{F}} < \tau \|\mathbf{x}_{\text{init}}\mathbf{x}_{\text{init}}^H - \mathbf{x}\mathbf{x}^H\|_{\mathcal{F}}, \quad (40)$$

for some $\tau \in (0, 1)$.

Proof: See Appendix B. ■

The initialization procedures in previous studies [47] usually relied on constructing a *fixed* matrix to approximate the correlation matrix $\mathbf{x}\mathbf{x}^H$ of the signal itself, and then extracting its principal eigenvector (with appropriate normalization). However, in our initialization procedure, such a matrix \mathbf{G}_ℓ is obtained iteratively. In [49], initialization similar to ours was employed for FROG PR but it lacked any performance guarantees.

V. NUMERICAL EXPERIMENTS

We validated our models and methods through extensive numerical experiments. We examine the ability of Algorithm 1 to recover the band- and time-limited signals from complete and incomplete data in both noiseless and noisy settings. The radar function is incomplete when only few shifts or Fourier frequencies are considered. Here, we define the SNR = $10 \log_{10}(\|\mathbf{A}\|_{\mathcal{F}}^2 / \|\boldsymbol{\sigma}\|_2^2)$, where $\boldsymbol{\sigma}$ is the variance

of the noise. The signals used in the simulations were constructed as follows. For all tests, we built a set of $\lceil \frac{N-1}{2} \rceil$ -band-limited and time-limited signals that conform to a Gaussian power spectrum centered at 800 Hz. Specifically, each signal ($N = 128$ grid points) is produced via the Fourier transform of a complex vector with a Gaussian-shaped amplitude with a cutoff frequency of 150 microseconds⁻¹ (usec⁻¹). Next, we multiply the obtained power spectrum by a uniformly distributed random phase. We used the inverse Fourier transform of this signal as the underlying (original) signal. From radar engineering perspective, these parameters correspond to a generic high-resolution system.

Throughout the experiments, we used the following parameters for Algorithm 1: $\gamma_1 = 0.1$, $\gamma = 0.1$, $\alpha = 0.6$, $\mu_0 = 65$, and $\epsilon = 1 \times 10^{-101}$. The number of indices chosen uniformly at random were set to $Q = N$.

Signal reconstruction from complete AF: Figs. 2 and 3 show the recovery of time and band-limited signals from a given complete AF in noiseless and noisy settings, respectively. For the latter, the radar AF trace is corrupted by Gaussian noise with SNR = 20 dB. Here, the “noisy” AF implies that AF is not perfectly designed thus allowing us to evaluate the robustness of Algorithm 1. A comparison of estimated signals with the original using the error metric as defined by (6) in the results of Figs. 2 and 3 suggests near-perfect recovery using Algorithm 1.

Signal reconstruction from uniformly undersampled AF: Figs. 4 and 5 show the estimated time- and band-limited signals from a noisy AF in which 50% and 75% of the delays were removed, respectively. Here, the delays were performed uniformly. For instance, in case of 50% removal, every two delays starting from the first one are preserved. Similarly, in case of 75% removal, one out of every four delays starting from the first one is preserved; this implies a total of 32 delays are used from the available 128 points. These results numerically validate Proposition 1 and Corollary 1) that all delays may not be required to estimate the underlying signal. We observe that Algorithm 1 is able to return a close estimation of the signal even when the incomplete AF is assumed imperfectly designed in Figs. 4 and 5. This further suggests robust performance of Algorithm 1.

Signal reconstruction from randomly undersampled AF: Next, we evaluated the performance of Algorithm 1 when some delays as well as the Doppler frequencies in the AF were non-uniformly removed. Figs. 6 and 7 show the recovery performance when 25% of the first and last (i.e., a total of 50%) delays and frequencies, respectively, of the AF were set to zero. A higher relative error in the results of Fig. 6 suggests that a non-uniform selection of the removed delays reduces the ability of Algorithm 1. On the other hand, the error does not increase significantly when frequencies are non-uniformly removed (Fig. 7).

Modulated signals: So far, we considered that the underlying signals are only time- or band-limited. We now impose an additional constraint of modulation, i.e. LFM and NLFM, to investigate the performance of Algorithm 1. These signals are very commonly used by radar systems [2]. We model these signals as

$$\mathbf{x}[n] = \mathbf{a}[n] e^{j\pi\varphi[n]}, \quad (41)$$

where

$$\mathbf{a}[n] = \begin{cases} 1 & 0 \leq \Delta tn \leq T \\ 0 & \text{otherwise} \end{cases}. \quad (42)$$

¹All simulations were implemented in Matlab R2019a on an Intel Core i7 3.41 Ghz CPU with 32 GB RAM.

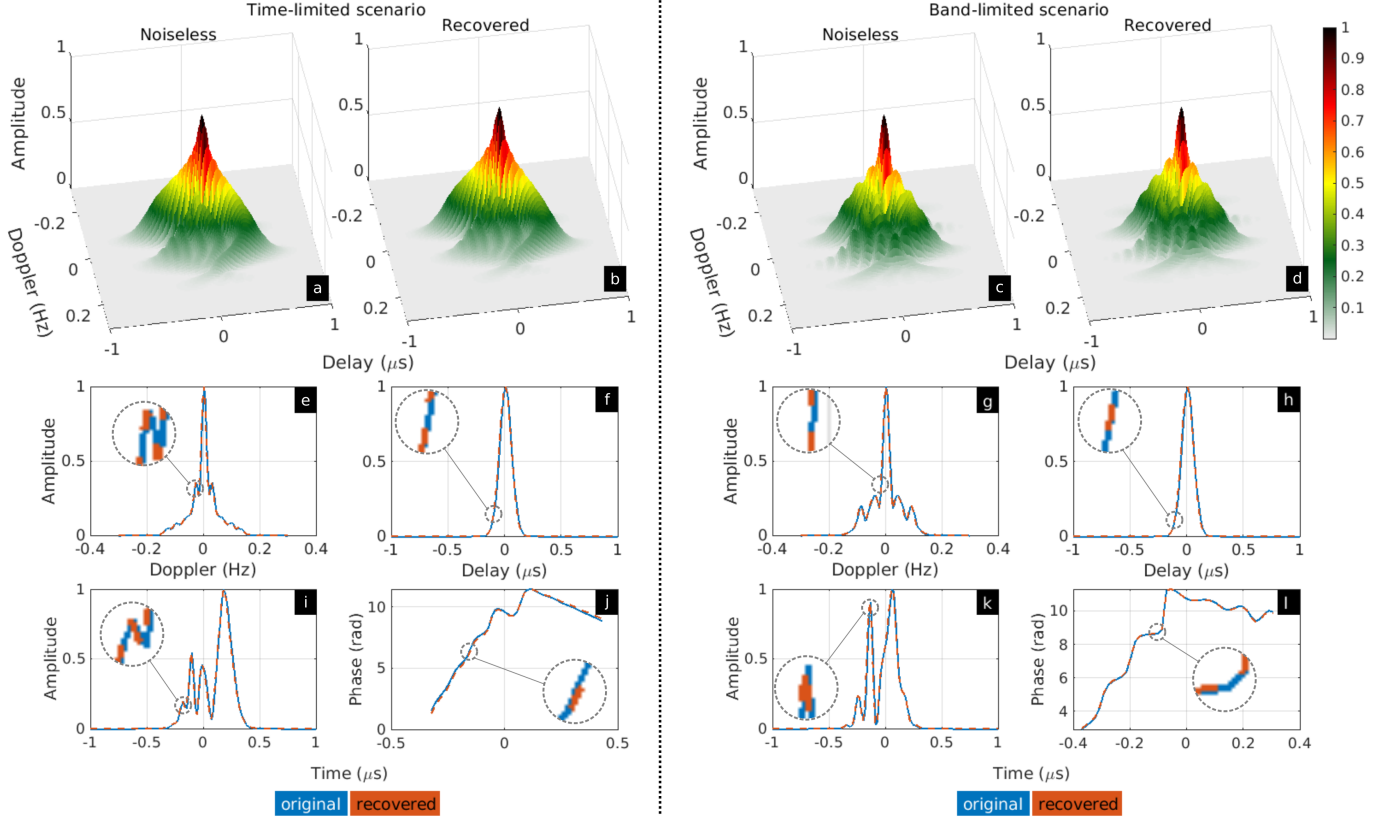


Fig. 2. Reconstructed time- and band-limited signals with their AFs in the absence of noise. In both cases, the attained relative error as defined by (6) is 1×10^{-6} . For time-limited [band-limited] signal, (a) [(c)] and (b) [(d)] show the original and recovered AFs, respectively; (e) [(g)] and (f) [(h)] are 1-D slices of the AFs at zero delay and Doppler, respectively; (i) [(k)] and (j) [(l)] are the, respectively, magnitude and phase of recovered (red) signal juxtaposed with the original (blue).

is a rectangular envelope, T as the duration of the pulse, Δt as the sampling size in time, and

$$\begin{aligned} \varphi[n] &= \pi k (\Delta t n)^2, & (\text{LFM}) \\ \varphi[n] &= \pi k t^2 + \sum_{l=1}^L \alpha_l \cos(2\pi l \Delta t n / T) & (\text{NLFM}), \end{aligned} \quad (43)$$

with $k = \frac{\Delta f}{T}$ such that Δf is the swept bandwidth and $L > 0$ is an integer. In this experiment, we use $\alpha_l = \frac{0.4T}{l}$, $\Delta f = 128 \times 10^3$, and $\Delta t = 0.4 \times 10^{-6}$.

We considered two noisy scenarios each with $SNR = 20$ dB. Fig. 8 shows the recovery performance for both LFM and NLFM signals when the 50% of the delays are uniformly removed from the AF. In Fig. 9, 19% of the first and last Fourier frequencies of the AF were removed. These results suggest that Algorithm 1 accurately estimates the phase of the pulses while the reconstructed magnitudes present some artifacts. This limitation comes from the fact that the LFM/NLFM AF is significantly wide such that the removed information is enough to degrade the reconstruction quality. **Statistical performance:** We evaluated the success rate of Algorithm 1 when the AF was incomplete. To this end, we initialized the algorithm at $\mathbf{x}^{(0)} = \mathbf{x} + \delta \zeta$, where δ is a fixed constant and ζ takes values on $\{-1, 1\}$ with equal probability, while a percentage of the removed delays were set to zero. A trial was declared successful when the returned estimate attains a relative error (defined by (6)) that is smaller than 10^{-6} . We numerically determined the empirical success rate over 100 trials. Fig. 10 summarizes these results for the case of time-limited signals and shows a high success rate of

Algorithm 1 even when a significant number of delays are removed from the AF.

Initialization procedure error: Finally, we examined the impact of our proposed initialization procedure in Algorithm 2 under noiseless (Fig. 11) and noisy (Fig. 12) scenarios. We compare the relative error between the initial vector in (29) and the returned solution $\mathbf{x}^{(0)}$ of the proposed method. The number of iterations to attain the vector $\mathbf{x}^{(0)}$ using the designed initialization was fixed to $T = 2$. We averaged the relative error over 100 trials. The results for both settings show that the proposed initialization algorithm outperforms \mathbf{x}_{init} .

VI. SUMMARY

There is a large body of literature on radar waveform design, including adapting existing waveforms for specialized tasks pertaining to detection, estimation, and tracking. Several non-AF-based waveform design techniques also exist (see [40] for a survey), in which the waveform is optimized to obey the specific SNR or sidelobe levels. However, modern agile radar systems require arbitrarily designing the transmit waveform to meet very specific AF performance requirements. Whereas prior works applied the classical Gerchberg-Saxton PR algorithm to Sussman's least-squares synthesis [31] of waveforms from their AFs, the convergence and recovery guarantees are inferior. Hence, it is beneficial to investigate recent advances in PR for AF-based signal recovery.

In this context, we analytically demonstrated that time/band-limited signals can be perfectly estimated (up to trivial ambiguities) from their (phaseless) AF. Our proposed trust-region gradient method estimated these signals under complete/incomplete and noisy/noiseless

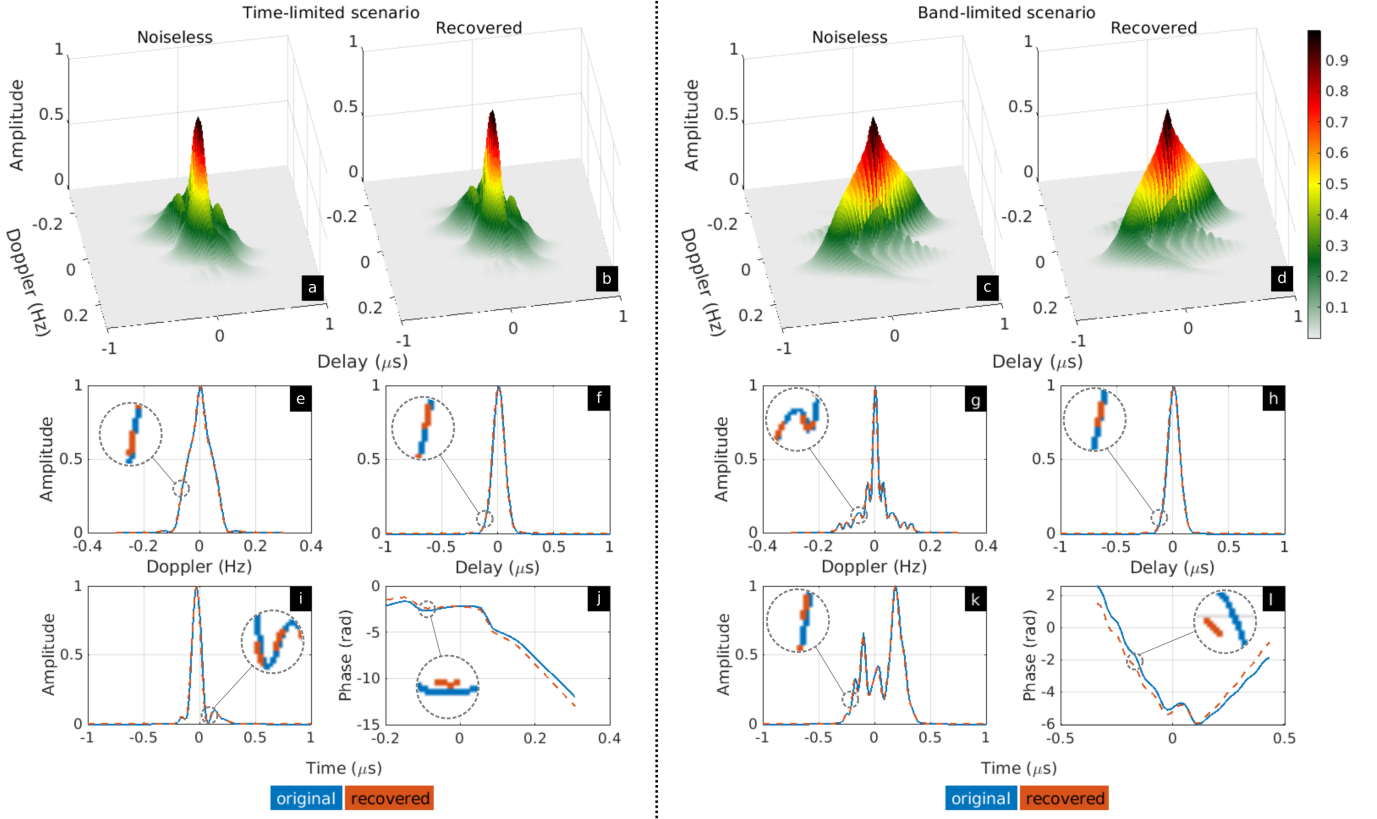


Fig. 3. As in Fig. 2 but in the presence of noise with $\text{SNR} = 20$ dB. The attained relative error is 5×10^{-2} for both time- and band-limited signals.

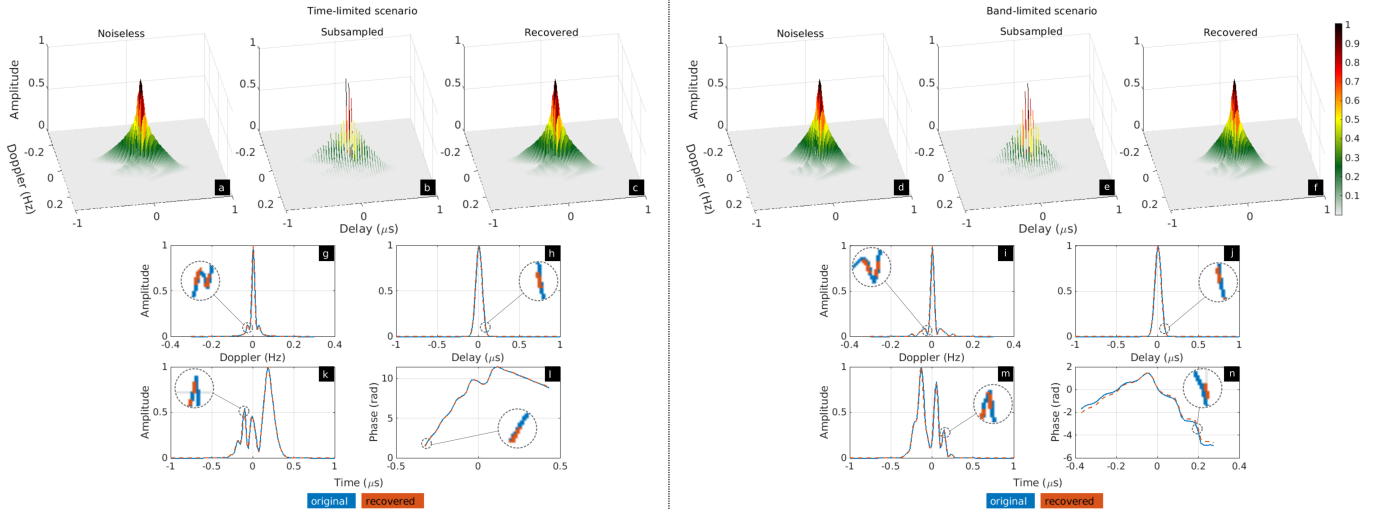


Fig. 4. As in Fig. 2 but in the presence of noise with $\text{SNR} = 20$ dB and with 50% of the delays uniformly removed from the AF. The attained relative error is 5×10^{-2} for both time- and band-limited signals. Additionally, For time-limited [band-limited] signal, (a) [(d)], (b) [(e)], and (c) [(f)] show the original, undersampled, and recovered AFs, respectively; (g) [(i)] and (h) [(j)] are 1-D slices of the AFs at zero delay and Doppler, respectively; (k) [(m)] and (l) [(n)] are the, respectively, magnitude and phase of recovered (red) signal juxtaposed with the original (blue).

scenarios. We verified the recovery in polynomial time with sufficient accuracy for complete AF. In particular, our new spectral initialization method suggested substantial performance enhancement.

In the case of incomplete data, whereas Proposition 1 and Corollary 1 suggested that full AF is not required to guarantee uniqueness, more work is required in future to better estimate the pulses from

incomplete data. Numerical results indicate that signals with wider AFs may not be retrieved accurately in undersampled scenario. The initialization strategy employed may also be improved. The AF-based PR optimization problem is highly non-convex for which we use an alternating approach. Hence, the presence of saddle points and local minimum should be avoided. We fixed the algorithmic parameters

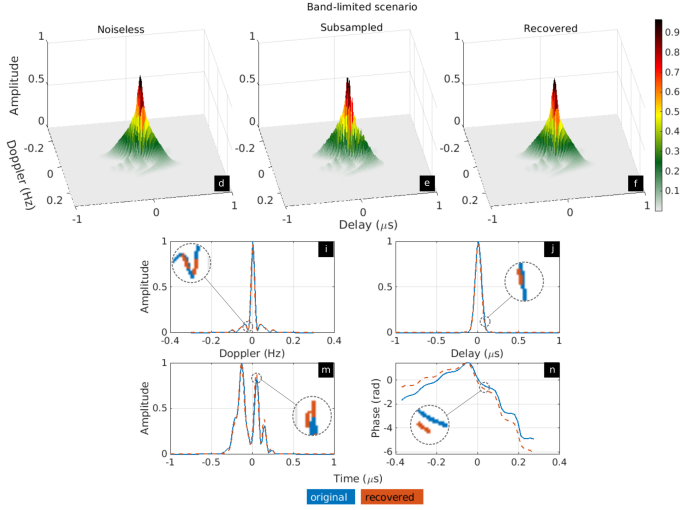
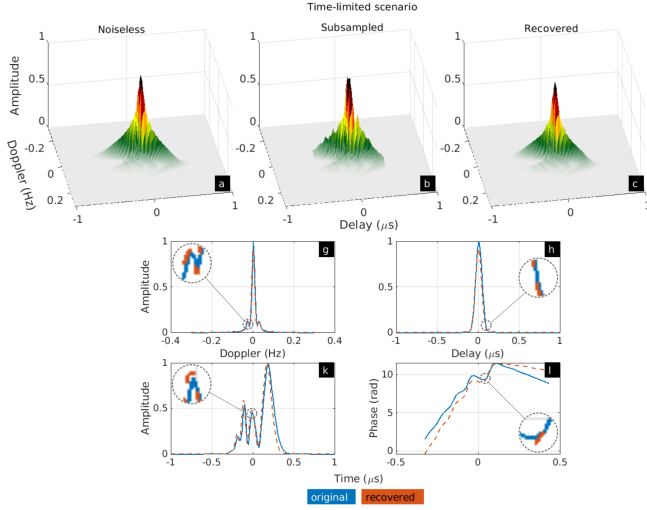


Fig. 5. As in Fig. 4 but with 75% of the delays uniformly removed from the AF. The attained relative error is 5×10^{-2} for both time- and band-limited signals.

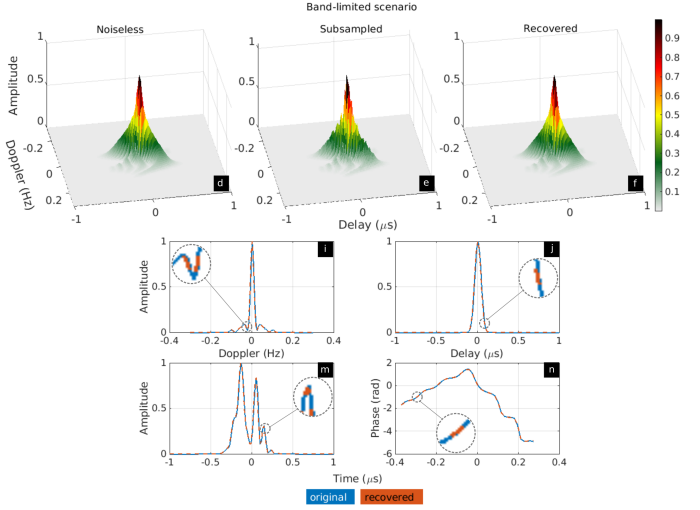
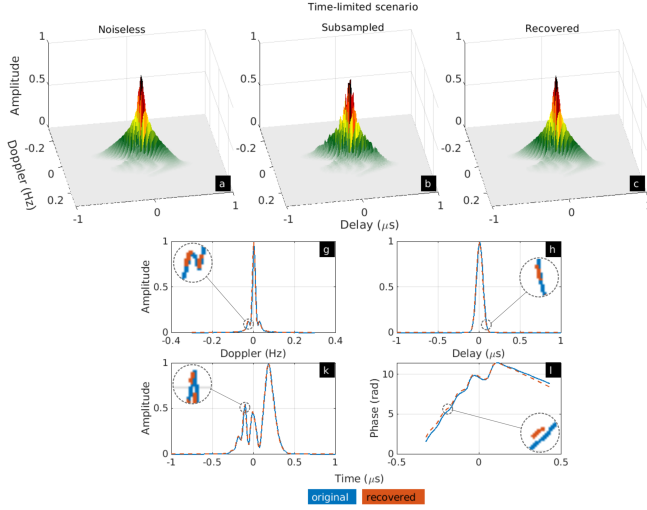


Fig. 6. As in Fig. 4 but with 50% of the delays non-uniformly removed from the AF. The attained relative error is 9×10^{-2} for both time- and band-limited signals.

through hit-and-trial but they may also be learned from the kind of signals. Finally, as we mentioned in the beginning, we remark that AF is not unique in definition. Therefore, generalization of this work to other more complex definitions will provide critical insights in apply PR theory to AF-based signal design.

APPENDIX A PROOF OF THEOREM 1

A. Preliminaries to the Proof

Define the search set as

$$\mathcal{J} := \{\mathbf{z} \in \mathbb{C}^N, B\text{-bandlimited} : \text{dist}(\mathbf{x}, \mathbf{z}) \leq \rho, B \leq N/2\}, \quad (44)$$

for some small constant $\rho > 0$. Recall that \mathbf{z} is a B -bandlimited signal if there exists k such that $\tilde{\mathbf{z}}[k] = \dots = \tilde{\mathbf{z}}[N+k+B-1] = 0$, where $\tilde{\mathbf{z}}$ is the Fourier transform of \mathbf{z} . The bandlimitedness guarantees that we have unique solution, according to Proposition 1. We first prove the

positivity of the product $|\mathbf{f}_k^H \mathbf{g}_p(\mathbf{z})|$ over the set \mathcal{J} in the following Lemma 3.

Lemma 3. Let $\mathbf{z} \in \mathcal{J}$ where \mathcal{J} as defined in (44). Then, for almost all $\mathbf{z} \in \mathcal{J}$ the following holds

$$|\mathbf{f}_k^H \mathbf{g}_p(\mathbf{z})| > 0, \quad (45)$$

for all $k, p \in \{0, \dots, N-1\}$, with

$$\mathbf{g}_p(\mathbf{z}) := [\mathbf{z}[0]\overline{\mathbf{z}[p]}, \dots, \mathbf{z}[N-1]\overline{\mathbf{z}[N-1+p]}]^T. \quad (46)$$

Proof: We prove this lemma by contradiction. Assume

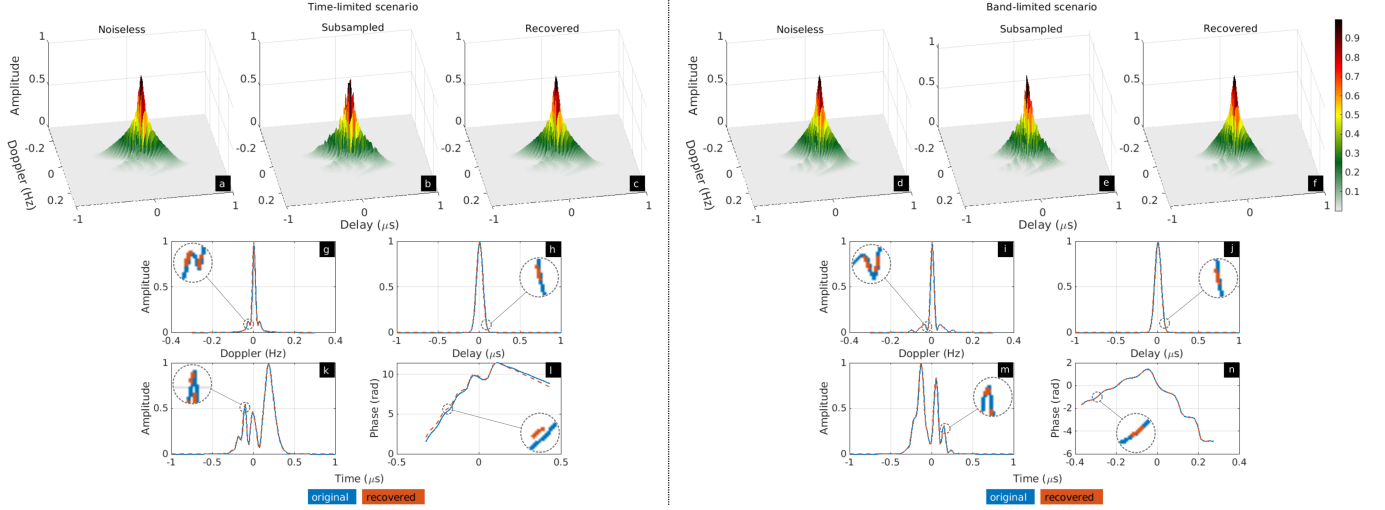


Fig. 7. As in Fig. 4 but with 50% of the Doppler frequencies non-uniformly removed from the AF. The attained relative error is 6×10^{-2} for both time- and band-limited signals.

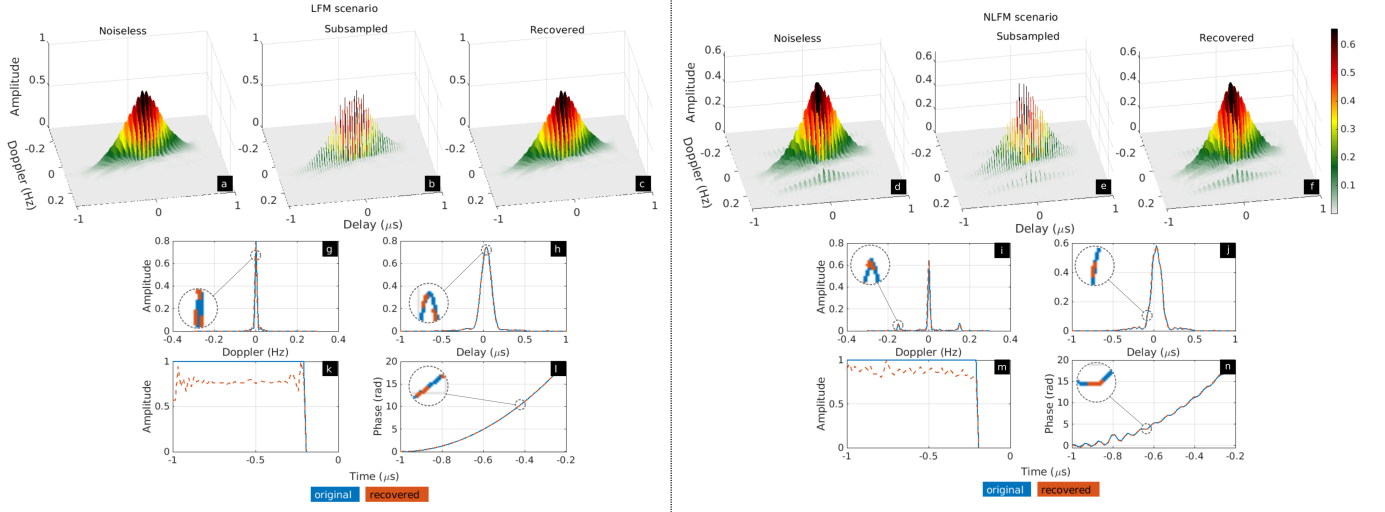


Fig. 8. As in Fig. 4 but time- and band-limited cases replaced by LFM and NLFM signals. The attained relative error is 6×10^{-2} for both time- and band-limited signals.

$|\mathbf{f}_k^H \mathbf{g}_p(\mathbf{z})| = 0$. Then, from (5) we have that

$$\begin{aligned} |\mathbf{f}_k^H \mathbf{g}_p(\mathbf{z})|^2 &= \left| \sum_{n=0}^{N-1} \mathbf{z}[n] \overline{\mathbf{z}[n-p]} e^{-2\pi i n k / N} \right|^2 \\ &= \sum_{n,m=0}^{N-1} \left(\mathbf{z}[n] \overline{\mathbf{z}[n-p]} \mathbf{z}[m-p] \overline{\mathbf{z}[m]} \right) e^{\frac{2\pi i (m-n)k}{N}} = 0. \end{aligned} \quad (47)$$

Note that (47) is a quartic polynomial equation with respect to the entries of \mathbf{z} . However, for almost all signals $\mathbf{z} \in \mathcal{J}$ the left hand side of (47) will not be equal to zero which leads to a contradiction. ■

In order to prove Theorem 1, the function $h(\mathbf{z}, \mu)$ in (15) must satisfy the four requirements stated in the following Lemma 4. These conditions are used in the analysis of convergence for stochastic gradient methods [65].

Lemma 4. The function $h(\mathbf{z}, \mu)$ in (15) and its Wirtinger derivative in (22) satisfy the following properties.

C1 The cost function $h(\mathbf{z}, \mu)$ in (15) is bounded below.

C2 The set \mathcal{J} as defined in (44) is closed and bounded.

C3 There exists a constant $U > 0$, such that

$$\left\| \frac{\partial h(\mathbf{z}_1, \mu)}{\partial \bar{\mathbf{z}}} - \frac{\partial h(\mathbf{z}_2, \mu)}{\partial \bar{\mathbf{z}}} \right\|_2 \leq U \|\mathbf{z}_1 - \mathbf{z}_2\|_2, \quad (48)$$

holds for all $\mathbf{z}_1, \mathbf{z}_2 \in \mathcal{J}$.

C4 For all $\mathbf{z} \in \mathcal{J}$

$$\mathbb{E}_{\Gamma(t)} \left[\left\| \mathbf{d}_{\Gamma(t)} - \frac{\partial h(\mathbf{z}, \mu)}{\partial \bar{\mathbf{z}}} \right\|_2^2 \right] \leq \zeta^2, \quad (49)$$

for some $\zeta > 0$, where $\mathbf{d}_{\Gamma(t)}$ is as in line 7 of Algorithm 1.

Proof:

To prove **C1**, from the definition of $h(\mathbf{z}, \mu)$ in (15), it follows that $h(\mathbf{z}, \mu) \geq 0$ and thus bounded below.

The property **C2** holds by definition.

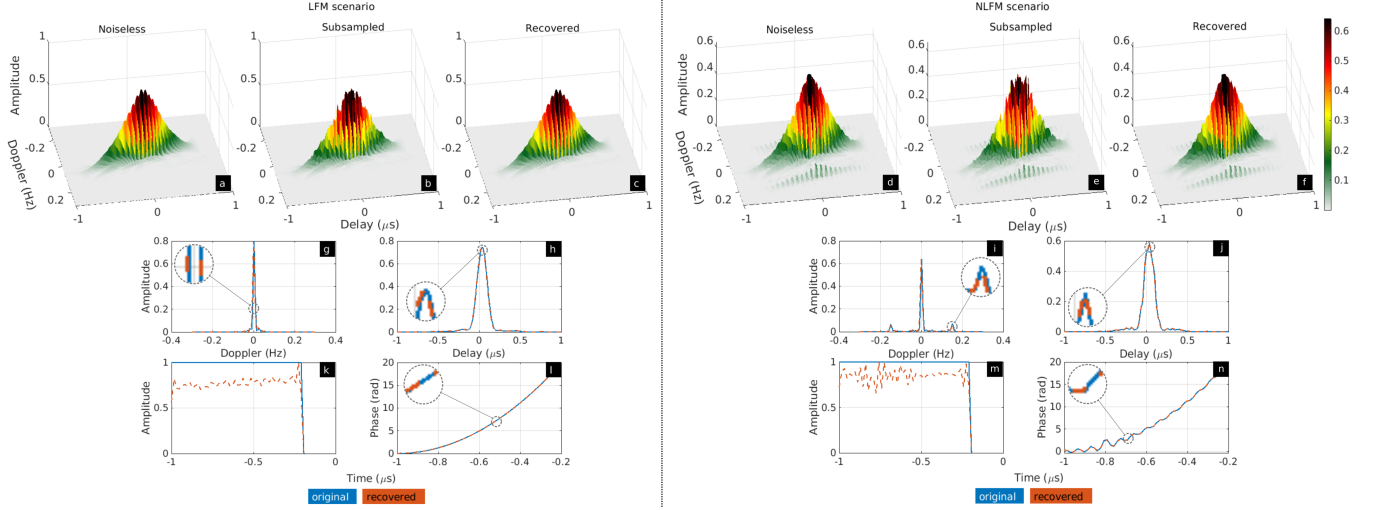


Fig. 9. As in Fig. 8 but with 19% of the first and last Doppler frequencies of the AFs removed. The attained relative error is 9×10^{-2} for both time- and band-limited signals.

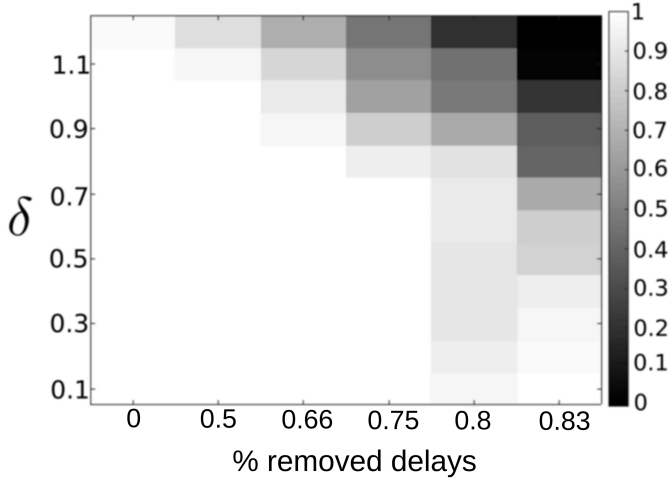


Fig. 10. Empirical success rate of Algorithm 1 as a function of % removed delays (uniformly) and δ in the absence of noise.

Regarding C3, it follows from (21) that ℓ -th entry of $\frac{\partial h(\mathbf{z}, \mu)}{\partial \bar{\mathbf{z}}}$ is

$$\begin{aligned} \frac{\partial h(\mathbf{z}, \mu)}{\partial \bar{\mathbf{z}}}[\ell] &= \frac{1}{N^2} \sum_{k,p=0}^{N-1} \left(\mathbf{f}_k^H \mathbf{g}_p(\mathbf{z}) - v_{k,p} \right) \mathbf{z}[\ell - p] e^{2\pi i \ell k / N} \\ &+ \frac{1}{N^2} \sum_{k,p=0}^{N-1} \left(\mathbf{f}_k^T \bar{\mathbf{g}}_p - v_{k,p} \right) \mathbf{z}[\ell + p] e^{-2\pi i (\ell + p) k / N}. \end{aligned} \quad (50)$$

Define $\mathbf{D}_p(\mathbf{z}) \in \mathbb{C}^{N \times N}$ as a diagonal matrix whose main diagonal is formed by the vector $\mathbf{z}_p = [\mathbf{z}_p[0], \dots, \mathbf{z}_p[N-1]]^T = [\mathbf{z}[-p], \dots, \mathbf{z}[N-1-p]]^T$. Thus,

$$\frac{\partial h(\mathbf{z}, \mu)}{\partial \bar{\mathbf{z}}} = \frac{1}{N^2} \sum_{p,k=0}^{N-1} f_{k,p}(\mathbf{z}) + g_{k,p}(\mathbf{z}), \quad (51)$$

$$\text{where } f_{k,p}(\mathbf{z}) = \rho_{k,p}(\mathbf{z}) \mathbf{D}_p(\mathbf{z}) \mathbf{f}_k, \quad g_{k,p}(\mathbf{z}) =$$

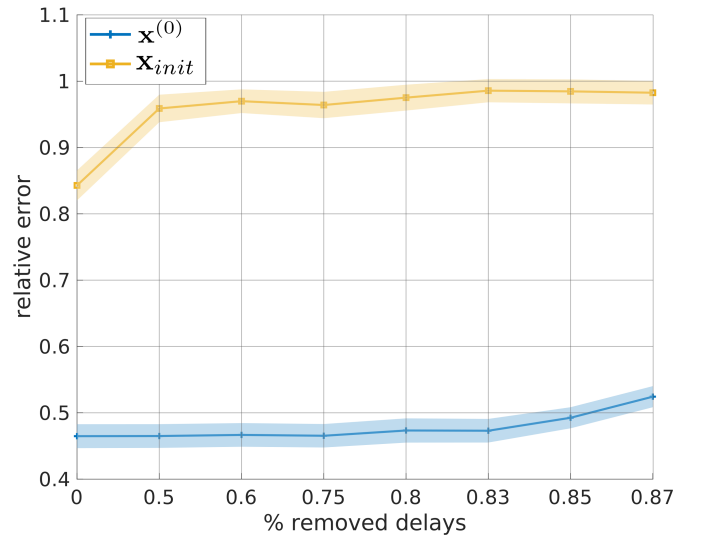


Fig. 11. Relative error comparison between the initial vector \mathbf{x}_{init} as defined in (29), and the returned initial guess $\mathbf{x}^{(0)}$ for different percentages of (uniformly) removed delays in a noiseless setting. The relative error was averaged over 100 trials.

$$\omega^{-kp} \overline{\rho_{k,p}(\mathbf{z})} \mathbf{D}_{-p}(\mathbf{z}) \mathbf{f}_k, \text{ and}$$

$$\rho_{k,p}(\mathbf{z}) = \mathbf{f}_k^H \mathbf{g}_p(\mathbf{z}) - \sqrt{\mathbf{A}[p, k]} \frac{\mathbf{f}_k^H \mathbf{g}_p(\mathbf{z})}{\varphi_\mu(|\mathbf{f}_k^H \mathbf{g}_p(\mathbf{z})|)}. \quad (52)$$

We now establish that, for all $\mathbf{z}_1, \mathbf{z}_2 \in \mathcal{J}$ and some constants $r_{k,p}, s_{k,p} > 0$, any $f_{k,p}(\mathbf{z})$ and $g_{k,p}(\mathbf{z})$ satisfy

$$\|f_{k,p}(\mathbf{z}_1) - f_{k,p}(\mathbf{z}_2)\|_2 \leq r_{k,p} \|\mathbf{z}_1 - \mathbf{z}_2\|_2, \quad (53)$$

and

$$\|g_{k,p}(\mathbf{z}_1) - g_{k,p}(\mathbf{z}_2)\|_2 \leq s_{k,p} \|\mathbf{z}_1 - \mathbf{z}_2\|_2. \quad (54)$$

We show only (53); the proof for $g_{k,p}(\mathbf{z})$ follows *mutatis mutandis*.

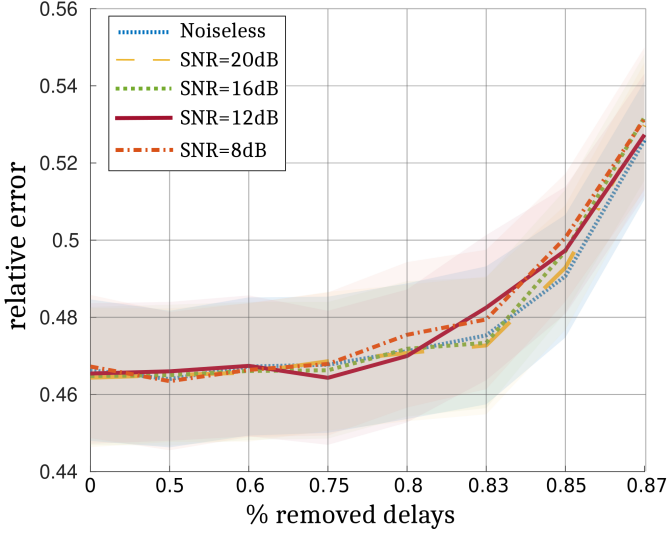


Fig. 12. Performance of the proposed initialization (Algorithm 2) for different SNR values as the (uniformly) removed delays are increased. The relative error was averaged over 100 trials.

Considering the fact that $\mathbf{D}_p(\mathbf{z}_1)$ and $\mathbf{D}_p(\mathbf{z}_2)$ are diagonal matrices and $\|\mathbf{f}_k\|_2 = \sqrt{N}$, it follows from the definition of $f_{k,p}(\mathbf{z})$ that, for any $\mathbf{z}_1, \mathbf{z}_2 \in \mathcal{J}$,

$$\frac{1}{\sqrt{N}} \|f_{k,p}(\mathbf{z}_1) - f_{k,p}(\mathbf{z}_2)\|_2 \leq \|\rho_{k,p}(\mathbf{z}_1)\bar{\mathbf{z}}_1 - \rho_{k,p}(\mathbf{z}_2)\bar{\mathbf{z}}_2\|_2, \quad (55)$$

Using (52) in the right-hand-side of (55) yields

$$\begin{aligned} & \|\rho_{k,p}(\mathbf{z}_1)\bar{\mathbf{z}}_1 - \rho_{k,p}(\mathbf{z}_2)\bar{\mathbf{z}}_2\|_2 \\ &= \|\rho_{k,p}(\mathbf{z}_1)(\bar{\mathbf{z}}_1 + \bar{\mathbf{z}}_2 - \bar{\mathbf{z}}_2) - \rho_{k,p}(\mathbf{z}_2)\bar{\mathbf{z}}_2\|_2 \\ &= \|\rho_{k,p}(\mathbf{z}_1)(\bar{\mathbf{z}}_1 - \bar{\mathbf{z}}_2) + \rho_{k,p}(\mathbf{z}_1)\bar{\mathbf{z}}_2 - \rho_{k,p}(\mathbf{z}_2)\bar{\mathbf{z}}_2\|_2 \\ &\leq \|\rho_{k,p}(\mathbf{z}_1)\| \|\bar{\mathbf{z}}_1 - \bar{\mathbf{z}}_2\|_2 + \|\bar{\mathbf{z}}_2\|_2 \|\rho_{k,p}(\mathbf{z}_1) - \rho_{k,p}(\mathbf{z}_2)\| \\ &= \frac{|\mathbf{f}_k^H \mathbf{g}_p(\mathbf{z}_1)|}{\varphi_\mu(|\mathbf{f}_k^H \mathbf{g}_p(\mathbf{z}_1)|)} \left| \varphi_\mu(|\mathbf{f}_k^H \mathbf{g}_p(\mathbf{z}_1)|) - \sqrt{\mathbf{A}[p, k]} \right| \|\mathbf{z}_1 - \mathbf{z}_2\|_2 \\ &\quad + \|\bar{\mathbf{z}}_2\|_2 \|\rho_{k,p}(\mathbf{z}_1) - \rho_{k,p}(\mathbf{z}_2)\|. \end{aligned} \quad (56)$$

Then, combining (56) with the inequality $\varphi_\mu(|\mathbf{f}_k^H \mathbf{g}_p(\mathbf{z}_1)|) \geq \mu$, (55) becomes

$$\begin{aligned} & \frac{1}{\sqrt{N}} \|f_{k,p}(\mathbf{z}_1) - f_{k,p}(\mathbf{z}_2)\|_2 \\ &\leq \frac{|\mathbf{f}_k^H \mathbf{g}_p(\mathbf{z}_1)|}{\mu} \left(\varphi_\mu(|\mathbf{f}_k^H \mathbf{g}_p(\mathbf{z}_1)|) + \sqrt{\mathbf{A}[p, k]} \right) \|\mathbf{z}_1 - \mathbf{z}_2\|_2 \\ &\quad + \underbrace{\|\bar{\mathbf{z}}_2\|_2 \|\rho_{k,p}(\mathbf{z}_1) - \rho_{k,p}(\mathbf{z}_2)\|}_{=p_1}. \end{aligned} \quad (57)$$

The term p_1 in (57) is upper bounded as

$$\begin{aligned} p_1 &= \left| \mathbf{f}_k^H \mathbf{g}_p(\mathbf{z}_1) \left(1 - \frac{\sqrt{\mathbf{A}[p, k]}}{\varphi_\mu(|\mathbf{f}_k^H \mathbf{g}_p(\mathbf{z}_1)|)} \right) \right. \\ &\quad \left. - \mathbf{f}_k^H \mathbf{g}_p(\mathbf{z}_2) \left(1 - \frac{\sqrt{\mathbf{A}[p, k]}}{\varphi_\mu(|\mathbf{f}_k^H \mathbf{g}_p(\mathbf{z}_2)|)} \right) \right| \\ &\leq \left| \mathbf{f}_k^H \mathbf{g}_p(\mathbf{z}_1) - \mathbf{f}_k^H \mathbf{g}_p(\mathbf{z}_2) \right| \\ &\quad + \sqrt{\mathbf{A}[p, k]} \left| \frac{\mathbf{f}_k^H \mathbf{g}_p(\mathbf{z}_1)}{\varphi_\mu(|\mathbf{f}_k^H \mathbf{g}_p(\mathbf{z}_1)|)} - \frac{\mathbf{f}_k^H \mathbf{g}_p(\mathbf{z}_2)}{\varphi_\mu(|\mathbf{f}_k^H \mathbf{g}_p(\mathbf{z}_2)|)} \right| \\ &= \left| \mathbf{f}_k^H \mathbf{g}_p(\mathbf{z}_1) - \mathbf{f}_k^H \mathbf{g}_p(\mathbf{z}_2) \right| \\ &\quad + \sqrt{\mathbf{A}[p, k]} \left| \frac{\mathbf{f}_k^H \mathbf{g}_p(\mathbf{z}_1) + \mathbf{f}_k^H \mathbf{g}_p(\mathbf{z}_2) - \mathbf{f}_k^H \mathbf{g}_p(\mathbf{z}_2)}{\varphi_\mu(|\mathbf{f}_k^H \mathbf{g}_p(\mathbf{z}_1)|)} \right. \\ &\quad \left. - \frac{\mathbf{f}_k^H \mathbf{g}_p(\mathbf{z}_2)}{\varphi_\mu(|\mathbf{f}_k^H \mathbf{g}_p(\mathbf{z}_2)|)} \right| \\ &\leq \left| \mathbf{f}_k^H \mathbf{g}_p(\mathbf{z}_1) - \mathbf{f}_k^H \mathbf{g}_p(\mathbf{z}_2) \right| \\ &\quad + \sqrt{\mathbf{A}[p, k]} \left| \frac{\mathbf{f}_k^H \mathbf{g}_p(\mathbf{z}_1) - \mathbf{f}_k^H \mathbf{g}_p(\mathbf{z}_2)}{\varphi_\mu(|\mathbf{f}_k^H \mathbf{g}_p(\mathbf{z}_1)|)} \right| \\ &\quad + \sqrt{\mathbf{A}[p, k]} \left| \frac{\mathbf{f}_k^H \mathbf{g}_p(\mathbf{z}_2)}{\varphi_\mu(|\mathbf{f}_k^H \mathbf{g}_p(\mathbf{z}_1)|)} - \frac{\mathbf{f}_k^H \mathbf{g}_p(\mathbf{z}_2)}{\varphi_\mu(|\mathbf{f}_k^H \mathbf{g}_p(\mathbf{z}_2)|)} \right| \\ &\leq \left| \mathbf{f}_k^H \mathbf{g}_p(\mathbf{z}_1) - \mathbf{f}_k^H \mathbf{g}_p(\mathbf{z}_2) \right| \\ &\quad + \frac{\sqrt{\mathbf{A}[p, k]}}{\mu^2} \varphi_\mu(|\mathbf{f}_k^H \mathbf{g}_p(\mathbf{z}_2)|) \left| \mathbf{f}_k^H \mathbf{g}_p(\mathbf{z}_1) - \mathbf{f}_k^H \mathbf{g}_p(\mathbf{z}_2) \right| \\ &\quad + \frac{\sqrt{\mathbf{A}[p, k]}}{\mu^2} \left| \mathbf{f}_k^H \mathbf{g}_p(\mathbf{z}_2) \right| \left| \varphi_\mu(|\mathbf{f}_k^H \mathbf{g}_p(\mathbf{z}_1)|) - \varphi_\mu(|\mathbf{f}_k^H \mathbf{g}_p(\mathbf{z}_2)|) \right|. \end{aligned} \quad (58)$$

Recall that, by Heine-Borel Theorem [66], \mathcal{J} is a closed bounded set, and thus compact. Since $\varphi_\mu(\cdot)$ is a continuous function, there exists a constant M_{φ_μ} such that $\varphi_\mu(|\mathbf{f}_k^H \mathbf{g}_p(\mathbf{z})|) \leq M_{\varphi_\mu}$ for all $\mathbf{z} \in \mathcal{J}$. Also, from [60, Lemma 2] we have that $\varphi_\mu(\cdot)$ is a 1-Lipschitz function. Combining this with (58) yields

$$\begin{aligned} p_1 &\leq \left| \mathbf{f}_k^H \mathbf{g}_p(\mathbf{z}_1) - \mathbf{f}_k^H \mathbf{g}_p(\mathbf{z}_2) \right| \\ &\quad + \frac{\sqrt{\mathbf{A}[p, k]} M_{\varphi_\mu}}{\mu^2} \left| \mathbf{f}_k^H \mathbf{g}_p(\mathbf{z}_1) - \mathbf{f}_k^H \mathbf{g}_p(\mathbf{z}_2) \right| \\ &\quad + \frac{\sqrt{\mathbf{A}[p, k]}}{\mu^2} \left| \mathbf{f}_k^H \mathbf{g}_p(\mathbf{z}_2) \right| \left| \left| \mathbf{f}_k^H \mathbf{g}_p(\mathbf{z}_1) \right| - \left| \mathbf{f}_k^H \mathbf{g}_p(\mathbf{z}_2) \right| \right| \\ &\leq \left(\frac{\sqrt{\mathbf{A}[p, k]} M_{\varphi_\mu}}{\mu^2} + 1 \right) \left| \mathbf{f}_k^H \mathbf{g}_p(\mathbf{z}_1) - \mathbf{f}_k^H \mathbf{g}_p(\mathbf{z}_2) \right| \\ &\quad + \frac{\sqrt{\mathbf{A}[p, k]}}{\mu^2} \left| \mathbf{f}_k^H \mathbf{g}_p(\mathbf{z}_2) \right| \left| \mathbf{f}_k^H \mathbf{g}_p(\mathbf{z}_1) - \mathbf{f}_k^H \mathbf{g}_p(\mathbf{z}_2) \right|, \end{aligned} \quad (59)$$

where the second inequality follows from the reverse triangle inequality. Using (59) in (57) gives

$$\begin{aligned} & \frac{1}{\sqrt{N}} \|f_{k,p}(\mathbf{z}_1) - f_{k,p}(\mathbf{z}_2)\|_2 \\ &\leq \frac{|\mathbf{f}_k^H \mathbf{g}_p(\mathbf{z}_1)|}{\mu} \left(M_{\varphi_\mu} + \sqrt{\mathbf{A}[p, k]} \right) \|\mathbf{z}_1 - \mathbf{z}_2\|_2 \\ &\quad + \|\bar{\mathbf{z}}_2\|_2 \left(\frac{\sqrt{\mathbf{A}[p, k]} M_{\varphi_\mu}}{\mu^2} + 1 \right) \left| \mathbf{f}_k^H \mathbf{g}_p(\mathbf{z}_1) - \mathbf{f}_k^H \mathbf{g}_p(\mathbf{z}_2) \right| \\ &\quad + \frac{\|\bar{\mathbf{z}}_2\|_2 \sqrt{\mathbf{A}[p, k]}}{\mu^2} \left| \mathbf{f}_k^H \mathbf{g}_p(\mathbf{z}_2) \right| \left| \mathbf{f}_k^H \mathbf{g}_p(\mathbf{z}_1) - \mathbf{f}_k^H \mathbf{g}_p(\mathbf{z}_2) \right|. \end{aligned} \quad (60)$$

Observe that the upper bound in (60) directly depends on a term of the form $\mathbf{f}_k^H \mathbf{g}_p(\mathbf{z})$ for some $\mathbf{z} \in \mathcal{J}$, which might be zero. However,

from Lemma 3, $|\mathbf{f}_k^H \mathbf{g}_p(\mathbf{z})| > 0$ or, equivalently, $\mathbf{f}_k^H \mathbf{g}_p(\mathbf{z}) \neq 0$, for almost all $\mathbf{z} \in \mathcal{J}$.

We now proceed to bound the term $|\mathbf{f}_k^H \mathbf{g}_p(\mathbf{z})|$. From (5),

$$\begin{aligned} |\mathbf{f}_k^H \mathbf{g}_p(\mathbf{z})| &= \left| \sum_{n=0}^{N-1} \mathbf{z}[n] \overline{\mathbf{z}[n-p]} e^{-2\pi i n k / N} \right| \\ &\leq \sum_{n=0}^{N-1} |\mathbf{z}[n] \overline{\mathbf{z}[n-p]}| \leq N \|\mathbf{z}\|_2, \end{aligned} \quad (61)$$

where the second inequality follows from the norm inequalities $\|\mathbf{z}\|_1 \leq \sqrt{N} \|\mathbf{z}\|_2$ and $\|\mathbf{z}\|_2 \leq \sqrt{N} \|\mathbf{z}\|_\infty$. Combining (60) and (61) we get

$$\begin{aligned} &\frac{1}{\sqrt{N}} \|f_{k,p}(\mathbf{z}_1) - f_{k,p}(\mathbf{z}_2)\|_2 \\ &\leq \frac{N \|\mathbf{z}_1\|_2}{\mu} \left(M_{\varphi_\mu} + \sqrt{\mathbf{A}[p,k]} \right) \|\mathbf{z}_1 - \mathbf{z}_2\|_2 \\ &\quad + \|\mathbf{z}_2\|_2 \left(\frac{\sqrt{\mathbf{A}[p,k]} M_{\varphi_\mu}}{\mu^2} + 1 \right) |\mathbf{f}_k^H \mathbf{g}_p(\mathbf{z}_1) - \mathbf{f}_k^H \mathbf{g}_p(\mathbf{z}_2)| \\ &\quad + \frac{N \|\mathbf{z}_2\|_2^2 \sqrt{\mathbf{A}[p,k]}}{\mu^2} |\mathbf{f}_k^H \mathbf{g}_p(\mathbf{z}_1) - \mathbf{f}_k^H \mathbf{g}_p(\mathbf{z}_2)|. \end{aligned} \quad (62)$$

Next, we bound the term $|\mathbf{f}_k^H \mathbf{g}_p(\mathbf{z}_1) - \mathbf{f}_k^H \mathbf{g}_p(\mathbf{z}_2)|$ in (62). Again, from (5)

$$\begin{aligned} &|\mathbf{f}_k^H \mathbf{g}_p(\mathbf{z}_1) - \mathbf{f}_k^H \mathbf{g}_p(\mathbf{z}_2)| \\ &\leq \sum_{n=0}^{N-1} |\mathbf{z}_1[n] \overline{\mathbf{z}_1[n-p]} - \mathbf{z}_2[n] \overline{\mathbf{z}_2[n-p]}| \\ &\leq N (\|\mathbf{z}_1\|_2 + \|\mathbf{z}_2\|_2) \|\mathbf{z}_1 - \mathbf{z}_2\|_2, \end{aligned} \quad (63)$$

where the second inequality again relies on the norm inequalities. Combining (62) and (63) produces

$$\|f_{k,p}(\mathbf{z}_1) - f_{k,p}(\mathbf{z}_2)\|_2 \leq r_{k,p} \|\mathbf{z}_1 - \mathbf{z}_2\|_2, \quad (64)$$

where the constant $r_{k,p}$ is

$$\begin{aligned} r_{k,p} &= \frac{N \sqrt{N} \|\mathbf{z}_1\|_2}{\mu} \left(M_{\varphi_\mu} + \sqrt{\mathbf{A}[p,k]} \right) \\ &\quad + N \sqrt{N} (\|\mathbf{z}_1\|_2 + \|\mathbf{z}_2\|_2) \|\mathbf{z}_2\|_2 \left(\frac{\sqrt{\mathbf{A}[p,k]} M_{\varphi_\mu}}{\mu^2} + 1 \right) \\ &\quad + N^2 \sqrt{N} (\|\mathbf{z}_1\|_2 + \|\mathbf{z}_2\|_2) \frac{\|\mathbf{z}_2\|_2^2 \sqrt{\mathbf{A}[p,k]}}{\mu^2}. \end{aligned} \quad (65)$$

Since the set \mathcal{J} is bounded, then $\|\mathbf{z}\|_2 < \infty$ for all $\mathbf{z} \in \mathcal{J}$. Therefore, $0 < r_{k,p} < \infty$, and from (64) the result holds.

To prove **C4**, observe that

$$\begin{aligned} &\mathbb{E}_{\Gamma(t)} \left[\left\| \mathbf{d}_{\Gamma(t)} - \frac{\partial h(\mathbf{z}, \mu)}{\partial \bar{\mathbf{z}}} \right\|_2^2 \right] \\ &\leq \mathbb{E}_{\Gamma(t)} \left[2 \|\mathbf{d}_{\Gamma(t)}\|_2^2 \right] + 2 \left\| \frac{\partial h(\mathbf{z}, \mu)}{\partial \bar{\mathbf{z}}} \right\|_2^2, \end{aligned} \quad (66)$$

where the inequality follows from $\|\mathbf{w}_1 + \mathbf{w}_2\|_2^2 \leq 2(\|\mathbf{w}_1\|_2^2 + \|\mathbf{w}_2\|_2^2)$ for any $\mathbf{w}_1, \mathbf{w}_2 \in \mathbb{C}^N$. Combining (48) and (66) yields

$$\mathbb{E}_{\Gamma(t)} \left[\left\| \mathbf{d}_{\Gamma(t)} - \frac{\partial h(\mathbf{z}, \mu)}{\partial \bar{\mathbf{z}}} \right\|_2^2 \right] \leq \mathbb{E}_{\Gamma(t)} \left[2 \|\mathbf{d}_{\Gamma(t)}\|_2^2 \right] + 2U \|\mathbf{z}\|_2^2, \quad (67)$$

for some $U > 0$. Recall that $\Gamma(t)$ is sampled uniformly at random from all subsets of $\{1, \dots, N\} \times \{1, \dots, N\}$ with cardinality Q .

From the definition of $\mathbf{d}_{\Gamma(t)}$ in line 7 of Algorithm 1, we conclude that

$$\begin{aligned} \mathbb{E}_{\Gamma(t)} \left[2 \|\mathbf{d}_{\Gamma(t)}\|_2^2 \right] &\leq \frac{4Q}{N^2} \sum_{p,k=0}^{N-1} \|f_{k,p}(\mathbf{z}) + g_{k,p}(\mathbf{z})\|_2^2 \\ &\leq \frac{8Q}{N^2} \sum_{p,k=0}^{N-1} \|f_{k,p}(\mathbf{z})\|_2^2 + \|g_{k,p}(\mathbf{z})\|_2^2, \end{aligned} \quad (68)$$

where we use the inequality $\|\mathbf{w}_1 + \mathbf{w}_2\|_2^2 \leq 2(\|\mathbf{w}_1\|_2^2 + \|\mathbf{w}_2\|_2^2)$ for any $\mathbf{w}_1, \mathbf{w}_2 \in \mathbb{C}^N$. Since $f_{k,p}(\mathbf{z})$ and $g_{k,p}(\mathbf{z})$ satisfy (53) and (54), respectively. Hence, for some constants $r_{k,p}, s_{k,p} > 0$,

$$\mathbb{E}_{\Gamma(t)} \left[2 \|\mathbf{d}_{\Gamma(t)}\|_2^2 \right] \leq \frac{8Q \|\mathbf{z}\|_2^2}{N^2} \sum_{p,k=0}^{N-1} r_{k,p}^2 + s_{k,p}^2. \quad (69)$$

Thus, combining (67) and (69) yields

$$\mathbb{E}_{\Gamma(t)} \left[\left\| \mathbf{d}_{\Gamma(t)} - \frac{\partial h(\mathbf{z}, \mu)}{\partial \bar{\mathbf{z}}} \right\|_2^2 \right] \leq \zeta^2, \quad (70)$$

where

$$\zeta = \|\mathbf{z}\|_2 \sqrt{\frac{8Q}{N^2} \sum_{p,k=0}^{N-1} r_{k,p}^2 + s_{k,p}^2 + 2U}. \quad (71)$$

Note that $\zeta < \infty$ because the set \mathcal{J} is bounded. This completes the proof. \blacksquare

B. Proof of the Theorem

Denote the set $\mathcal{K}_1 := \{t | \mu^{(t+1)} = \gamma_1 \mu^{(t)}\}$, where $\gamma_1 \in (0, 1)$ is a tunable parameter [67]. If the set \mathcal{K}_1 is finite, then it follows from the lines 7-8 of Algorithm 1 that there exists an integer \hat{t} such that for all $t > \hat{t}$

$$\|\mathbf{d}_{\Gamma(t)}\|_2 \geq \gamma \mu^{(t)}, \quad (72)$$

with $\gamma \in (0, 1)$. Taking $\dot{\mu} = \mu^{(t)}$, the optimization problem (15) reduces to

$$\underset{\mathbf{z} \in \mathbb{C}^N}{\text{minimize}} \quad h(\mathbf{z}, \dot{\mu}). \quad (73)$$

Using the properties stated in Lemma 4, it follows from [65, Theorem 2.1] that

$$\lim_{t \rightarrow \infty} \left\| \frac{\partial h(\mathbf{x}^{(t)}, \mu^{(t)})}{\partial \bar{\mathbf{z}}} \right\|_2 = \lim_{t \rightarrow \infty} \left\| \mathbb{E}_{\Gamma(t)} [\mathbf{d}_{\Gamma(t)}] \right\|_2 = 0. \quad (74)$$

Clearly, (74) contradicts the assumption $\|\mathbf{d}_{\Gamma(t)}\|_2 \geq \gamma \mu^{(t)}$, for all $t > \hat{t}$. This shows that \mathcal{K}_1 must be infinite and $\lim_{t \rightarrow \infty} \mu^{(t)} = 0$.

Given that \mathcal{K}_1 is infinite, we deduce that

$$\begin{aligned} \lim_{t \rightarrow \infty} \left\| \frac{\partial h(\mathbf{x}^{(t)}, \mu^{(t)})}{\partial \bar{\mathbf{z}}} \right\|_2 &= \lim_{t \rightarrow \infty} \left\| \mathbb{E}_{\Gamma(t)} [\mathbf{d}_{\Gamma(t)}] \right\|_2 \\ &\leq \lim_{t \rightarrow \infty} \mathbb{E}_{\Gamma(t)} [\|\mathbf{d}_{\Gamma(t)}\|_2] \\ &\leq \gamma \lim_{t \rightarrow \infty} \mu^{(t)} = 0, \end{aligned} \quad (75)$$

where the second inequality follows from Jensen's inequality. This completes the proof.

APPENDIX B
PROOF OF THEOREM 2

Note that the function as defined in (36), i.e.

$$\mathbf{p}_\ell \rightarrow \|\mathbf{y}_\ell - \mathbf{G}_\ell^{(t-1)} \mathbf{p}_\ell\|_2^2 + \frac{1}{2\lambda_{(t)}} \|\mathbf{p}_\ell - \mathbf{x}_\ell^{(t-1)}\|_2^2$$

is $\frac{1}{\lambda_{(t)}}$ -strongly convex in \mathbf{p}_ℓ . Here, we allow inaccuracy in the solutions. More precisely, if we define $\mathbf{x}_{\ell,*}^{(t)}$ to be the exact minimizer of (36), the standard optimality conditions for strongly convex minimization imply that there exists a sequence of additive accuracy parameters $\epsilon_{(t)} \geq 0$ such that the numerically attained solution $\mathbf{x}_\ell^{(t)}$ satisfies

$$\begin{aligned} & \|\mathbf{y}_\ell - \mathbf{G}_\ell^{(t-1)} \mathbf{x}_\ell^{(t)}\|_2^2 + \frac{1}{2\lambda_{(t)}} \|\mathbf{x}_\ell^{(t)} - \mathbf{x}_\ell^{(t-1)}\|_2^2 \\ & \leq \|\mathbf{y}_\ell - \mathbf{G}_\ell^{(t-1)} \mathbf{x}_{\ell,*}^{(t)}\|_2^2 + \frac{1}{2\lambda_{(t)}} \|\mathbf{x}_{\ell,*}^{(t)} - \mathbf{x}_\ell^{(t-1)}\|_2^2 + \epsilon_{(t)} \\ & \leq \|\mathbf{y}_\ell - \mathbf{G}_\ell^{(t-1)} \mathbf{x}_\ell\|_2^2 + \frac{1}{2\lambda_{(t)}} \|\mathbf{x}_\ell - \mathbf{x}_\ell^{(t-1)}\|_2^2 + \epsilon_{(t)}, \end{aligned} \quad (76)$$

where \mathbf{x}_ℓ is the unknown desired signal and $\frac{1}{2\lambda_{(t)}} \|\mathbf{x}_\ell^{(t)} - \mathbf{x}_\ell\| \leq \epsilon_{(t)}$ [68]. Then, from (76),

$$\begin{aligned} \|\mathbf{y}_\ell - \mathbf{G}_\ell^{(t-1)} \mathbf{x}_\ell^{(t)}\|_2^2 & \leq \|\mathbf{y}_\ell - \mathbf{G}_\ell^{(t-1)} \mathbf{x}_\ell\|_2^2 \\ & + \frac{1}{2\lambda_{(t)}} \|\mathbf{x}_\ell - \mathbf{x}_\ell^{(t-1)}\|_2^2 + \epsilon_{(t)}. \end{aligned} \quad (77)$$

Recall that the radar PR problem has several ambiguities. In fact, the feasible set \mathcal{A}_ℓ for each ℓ is

$$\mathcal{A}_\ell = \{e^{j\beta} \mathbf{x}_\ell\} \cup \{\mathbf{x}_\ell[n-r]\} \cup \{\mathbf{x}_\ell[-n]\} \cup \{e^{ibn} \mathbf{x}_\ell[n]\}, \quad (78)$$

for all $r = 0, \dots, N-1$, and $b, \beta \in \mathbb{R}$. Thus, performing a parallel derivation with $\mathbf{q}_\ell^{(t-1)} \in \mathcal{A}_\ell$ replacing $\mathbf{x}_\ell^{(t-1)}$ and simplifying, we have from (76) and (77) that

$$\begin{aligned} \|\mathbf{y}_\ell - \mathbf{G}_\ell^{(t-1)} \mathbf{x}_\ell^{(t)}\|_2^2 & \leq \|\mathbf{y}_\ell - \mathbf{G}_\ell^{(t-1)} \mathbf{x}_\ell\|_2^2 \\ & + \frac{1}{2\lambda_{(t)}} \|\mathbf{x}_\ell + \mathbf{q}_\ell^{(t-1)}\|_2^2 + \epsilon_{(t)}. \end{aligned} \quad (79)$$

We rewrite the term at the left-hand-side of the inequality in (79) as

$$\begin{aligned} & \|\mathbf{y}_\ell - \mathbf{G}_\ell^{(t-1)} \mathbf{x}_\ell^{(t)}\|_2^2 \\ & = \|\mathbf{y}_\ell - \mathbf{G}_\ell^{(t-1)} \mathbf{x}_\ell^{(t)} - \mathbf{G}_\ell^{(t-1)} \mathbf{x}_\ell + \mathbf{G}_\ell^{(t-1)} \mathbf{x}_\ell\|_2^2 \\ & = \|\mathbf{y}_\ell - \mathbf{G}_\ell^{(t-1)} \mathbf{x}_\ell\|_2^2 + \|\mathbf{G}_\ell^{(t-1)} \mathbf{z}_\ell^{(t)} - \mathbf{G}_\ell^{(t-1)} \mathbf{x}_\ell\|_2^2 \\ & - 2\mathcal{R} \left(\left(\mathbf{y}_\ell - \mathbf{G}_\ell^{(t-1)} \mathbf{x}_\ell \right)^H \left(\mathbf{G}_\ell^{(t-1)} \mathbf{z}_\ell^{(t)} - \mathbf{G}_\ell^{(t-1)} \mathbf{x}_\ell \right) \right) \\ & \geq \|\mathbf{G}_\ell^{(t-1)} \mathbf{z}_\ell^{(t)} - \mathbf{G}_\ell^{(t-1)} \mathbf{x}_\ell\|_2^2 \\ & - 2 \left| \left(\mathbf{y}_\ell - \mathbf{G}_\ell^{(t-1)} \mathbf{x}_\ell \right)^H \left(\mathbf{G}_\ell^{(t-1)} \mathbf{x}_\ell^{(t)} - \mathbf{G}_\ell^{(t-1)} \mathbf{x}_\ell \right) \right| \\ & \geq \rho_1^{(t)} \|\mathbf{x}_\ell^{(t)} - \mathbf{x}_\ell\|_2^2 - 2\rho_2^{(t)} \|\mathbf{x}_\ell\|_2 \|\mathbf{x}_\ell^{(t)} - \mathbf{x}_\ell\|_2, \end{aligned} \quad (80)$$

where $\rho_1^{(t)}$ is the squared smallest singular value of $\mathbf{G}_\ell^{(t)}$ greater than zero, $\rho_2^{(t)} = \sigma_{\max} \left(\mathbf{G}_\ell - \mathbf{G}_\ell^{(t-1)} \right) \sigma_{\max} \left(\mathbf{G}_\ell^{(t-1)} \right)$. Then, combining (79) and (80) yields

$$\begin{aligned} \rho_1^{(t)} \|\mathbf{x}_\ell^{(t)} - \mathbf{x}_\ell\|_2^2 & \leq \frac{1}{2\lambda_{(t)}} \|\mathbf{x}_\ell + \mathbf{q}_\ell^{(t-1)}\|_2^2 \\ & + 2\rho_2^{(t)} \|\mathbf{x}_\ell\|_2 \|\mathbf{x}_\ell^{(t)} - \mathbf{x}_\ell\|_2 \\ & + \|\mathbf{y}_\ell - \mathbf{G}_\ell^{(t-1)} \mathbf{x}_\ell\|_2^2 + \epsilon_{(t)}. \end{aligned} \quad (81)$$

Considering the construction of matrix $\mathbf{G}_\ell^{(t-1)}$ in (16), we bound the term $\|\mathbf{G}_\ell - \mathbf{G}_\ell^{(t-1)}\|_{\mathcal{F}}^2$ in (81) as

$$\|\mathbf{G}_\ell - \mathbf{G}_\ell^{(t-1)}\|_{\mathcal{F}}^2 \leq 2N\lambda_{(t)}\epsilon_{(t-1)}, \quad (82)$$

because $\frac{1}{2\lambda_{(t-1)}} \|\mathbf{x}_\ell^{(t-1)} - \mathbf{x}_\ell\| \leq \epsilon_{(t-1)}$. Combining (81) and (82) produces

$$\begin{aligned} \rho_1^{(t)} \|\mathbf{x}_\ell^{(t)} - \mathbf{x}_\ell\|_2^2 & \leq \frac{1}{2\lambda_{(t)}} \|\mathbf{x}_\ell + \mathbf{q}_\ell^{(t-1)}\|_2^2 \\ & + 2\rho_2^{(t)} \|\mathbf{x}_\ell\|_2 \|\mathbf{x}_\ell^{(t)} - \mathbf{x}_\ell\|_2 \\ & + 2N\lambda_{(t)}\epsilon_{(t-1)} \|\mathbf{x}_\ell\|_2^2 + \epsilon_{(t)}. \end{aligned} \quad (83)$$

Note that the inequality (83) is valid for all trivial ambiguities of \mathbf{x}_ℓ for the radar problem. In particular, taking the minimum over the ambiguities of \mathbf{x}_ℓ on both sides of (83) implies

$$\begin{aligned} \rho_1^{(t)} \|\mathbf{x}_\ell^{(t)} - \mathbf{x}_\ell\|_2^2 & \leq \frac{1}{2\lambda_{(t)}} \|\mathbf{x}_\ell^{(t-1)} - \mathbf{x}_\ell\|_2^2 \\ & + 2N\lambda_{(t)}\epsilon_{(t-1)} \|\mathbf{x}_\ell\|_2^2 + \epsilon_{(t)} \end{aligned} \quad (84)$$

or

$$\begin{aligned} \|\mathbf{x}_\ell^{(t)} - \mathbf{x}_\ell\|_2^2 & \leq \frac{1}{2\lambda_{(t)}\rho_1^{(t)}} \|\mathbf{x}_\ell^{(t-1)} - \mathbf{x}_\ell\|_2^2 \\ & + 2N\lambda_{(t)}\epsilon_{(t-1)} \|\mathbf{x}_\ell\|_2^2 + \epsilon_{(t)}. \end{aligned} \quad (85)$$

Inductively applying the inequality (85) when $\epsilon_{(t)} = 0$ for all t yields

$$\|\mathbf{x}_\ell^{(t)} - \mathbf{x}_\ell\|_2 \leq \frac{1}{\sqrt{2\lambda_{(t)}\rho_1^{(t)}}} \|\mathbf{x}_\ell^{(t-1)} - \mathbf{x}_\ell\|_2, \quad (86)$$

wherein choosing $\lambda_{(t)}$ such that $\lambda_{(t)}\rho_1^{(t)} > 1/2$ guarantees a reduction in the estimation error of \mathbf{x}_ℓ . Then, from (86),

$$\|\mathbf{x}_\ell^{(t)} - \mathbf{x}_\ell\|_2 < \tau \|\mathbf{x}_\ell^{(0)} - \mathbf{x}_\ell\|_2, \quad (87)$$

where $\tau = \prod_t \frac{1}{\sqrt{2\lambda_{(t)}\rho_1^{(t)}}} < 1$.

Finally, using $\text{diag}(\mathbf{x}\mathbf{x}^H, \ell) = \mathbf{x}_\ell$, we obtain from (87) that

$$\|\mathbf{x}^{(0)}(\mathbf{x}^{(0)})^H - \mathbf{x}\mathbf{x}^H\|_{\mathcal{F}} < \tau \|\mathbf{x}_{\text{init}}\mathbf{x}_{\text{init}}^H - \mathbf{x}\mathbf{x}^H\|_{\mathcal{F}}, \quad (88)$$

where $\mathbf{x}^{(0)}$ is the returned vector of Algorithm 2, and \mathbf{x}_{init} as in (29). This completes the proof.

REFERENCES

- [1] N. Levanon, *Radar principles*. Wiley-Interscience, 1988.
- [2] P. Z. Peebles, *Radar principles*. Wiley-Interscience, 1998.
- [3] T. H. Glisson, C. I. Black, and A. P. Sage, "On sonar signal analysis," *IEEE Transactions on Aerospace and Electronic Systems*, no. 1, pp. 37–50, 1970.
- [4] J. Ville, "Théorie et application de la notion de signal analytique," *Câbles et transmissions*, vol. 2, no. 1, pp. 61–74, 1948, in French.
- [5] P. M. Woodward, *Probability and information theory, with applications to radar*, 3rd ed., ser. International Series of Monographs on Electronics and Instrumentation. McGraw-Hill, 1965.
- [6] —, "Radar ambiguity analysis," Royal Radar Establishment, Malvern, UK, Tech. Rep. RRE-TN-731, 1967.
- [7] W. Siebert, "A radar detection philosophy," *IRE Transactions on Information Theory*, vol. 2, no. 3, pp. 204–221, 1956.
- [8] C. Baylis, L. Cohen, D. Eustice, and R. Marks, "Myths concerning Woodward's ambiguity function: Analysis and resolution," *IEEE Transactions on Aerospace and Electronic Systems*, vol. 52, no. 6, pp. 2886–2895, 2016.
- [9] Y. I. Abramovich and G. J. Frazer, "Bounds on the volume and height distributions for the MIMO radar ambiguity function," *IEEE Signal Processing Letters*, vol. 15, pp. 505–508, 2008.
- [10] D. Swick, "An ambiguity function independent of assumptions about bandwidth and carrier frequency," Naval Research Laboratory, Washington DC, Tech. Rep., 1966.
- [11] J. Speiser, "Wide-band ambiguity functions," *IEEE Transactions on Information Theory*, vol. 13, no. 1, pp. 122–123, 1967.
- [12] D. Swick, "Wideband ambiguity function of pseudo-random sequences: An open problem," *IEEE Transactions on Information Theory*, vol. 14, no. 4, pp. 602–603, 1968.
- [13] R. J. Doviak and D. S. Zrnić, *Doppler radar and weather observations*, 2nd ed. Dover Publications, 2006.

- [14] J. George, K. V. Mishra, C. M. Nguyen, and V. Chandrasekar, "Implementation of blind zone and range-velocity ambiguity mitigation for solid-state weather radar," in *IEEE Radar Conference*, 2010, pp. 1434–1438.
- [15] R. Gassner and G. Cooper, "Note on a generalized ambiguity function," *IEEE Transactions on Information Theory*, vol. 13, no. 1, pp. 126–126, 1967.
- [16] B. Boashash, *Time-frequency signal analysis and processing: A comprehensive reference*. Academic Press, 2015.
- [17] R. de Buda, "An extension of Green's condition to cross-ambiguity functions," *IEEE Transactions on Information Theory*, vol. 13, no. 1, pp. 75–81, 1967.
- [18] G. San Antonio, D. R. Fuhrmann, and F. C. Robey, "MIMO radar ambiguity functions," *IEEE Journal of Selected Topics in Signal Processing*, vol. 1, no. 1, pp. 167–177, 2007.
- [19] C. V. Ilioudis, C. Clemente, I. K. Proudler, and J. Soraghan, "Generalized ambiguity function for MIMO radar systems," *IEEE Transactions on Aerospace and Electronic Systems*, vol. 55, no. 6, pp. 2629–2646, 2019.
- [20] J.-P. Guigay, "The ambiguity function in diffraction and isoplanatic imaging by partially coherent beams," *Optics Communications*, vol. 26, no. 2, pp. 136–138, 1978.
- [21] H. Bartelt, J. Ojeda-Castañeda, and E. E. Sicre, "Misfocus tolerance seen by simple inspection of the ambiguity function," *Applied Optics*, vol. 23, no. 16, pp. 2693–2696, 1984.
- [22] J. Ojeda-Castaneda, L. Berriel-Valdos, and E. Montes, "Ambiguity function as a design tool for high focal depth," *Applied Optics*, vol. 27, no. 4, pp. 790–795, 1988.
- [23] L. Auslander and R. Tolimieri, "Characterizing the radar ambiguity functions," *IEEE Transactions on Information theory*, vol. 30, no. 6, pp. 832–836, 1984.
- [24] B. R. Mahafza, *Radar systems analysis and design using MATLAB*. Chapman and Hall/CRC, 2005.
- [25] S. S. Soliman and R. A. Scholtz, "Spread ambiguity functions," *IEEE transactions on information theory*, vol. 34, no. 2, pp. 343–347, 1988.
- [26] M. Jankiraman, *Design of multi-frequency CW radars*. SciTech Publishing, 2007, vol. 2.
- [27] A. W. Rihaczek, *Principles of high-resolution radar*. Artech House, 1996.
- [28] D. DeLong and E. Hofstetter, "On the design of optimum radar waveforms for clutter rejection," *IEEE Transactions on Information Theory*, vol. 13, no. 3, pp. 454–463, 1967.
- [29] C. Stutt and L. Spafford, "A 'best' mismatched filter response for radar clutter discrimination," *IEEE Transactions on Information Theory*, vol. 14, no. 2, pp. 280–287, 1968.
- [30] C. H. Wilcox, "The synthesis problem for radar ambiguity functions," University of Wisconsin, Madison, WI, MRC Technical Summary Report 156, 1960.
- [31] S. Sussman, "Least-square synthesis of radar ambiguity functions," *IRE Transactions on Information Theory*, vol. 8, no. 3, pp. 246–254, 1962.
- [32] O. Arikan and D. Munson, "Time-frequency waveform synthesis using a least-squares approach," in *IEEE International Symposium on Circuits and Systems*, 1990, pp. 242–245.
- [33] S. Sen and A. Nehorai, "Adaptive design of OFDM radar signal with improved wideband ambiguity function," *IEEE Transactions on Signal Processing*, vol. 58, no. 2, pp. 928–933, 2009.
- [34] R. de Buda, "Signals that can be calculated from their ambiguity function," *IEEE Transactions on Information Theory*, vol. 16, no. 2, pp. 195–202, 1970.
- [35] K. Alhujaili, V. Monga, and M. Rangaswamy, "Quartic gradient descent for tractable radar slow-time ambiguity function shaping," *IEEE Transactions on Aerospace and Electronic Systems*, vol. 56, no. 2, pp. 1474–1489, 2019.
- [36] B. Nuss, J. Mayer, S. Marahrens, and T. Zwick, "Frequency comb OFDM radar system with high range resolution and low sampling rate," *IEEE Transactions on Microwave Theory and Techniques*, vol. 68, no. 9, pp. 3861–3871, 2020.
- [37] F. Rodriguez-Morales, C. Leuschen, C. Carabajal, J. Paden, J. A. Wolf, S. Garrison, and J. McDaniel, "An improved UWB microwave radar for very long-range measurements of snow cover," *IEEE Transactions on Instrumentation and Measurement*, vol. 69, no. 10, pp. 7761–7772, 2020.
- [38] P. Jaming, "The phase retrieval problem for the radar ambiguity function and vice versa," in *IEEE Radar Conference*, 2010, pp. 230–235.
- [39] E. J. Candés, X. Li, and M. Soltanolkotabi, "Phase retrieval from coded diffraction patterns," *Applied and Computational Harmonic Analysis*, vol. 39, no. 2, pp. 277–299, 2015.
- [40] H. He, J. Li, and P. Stoica, *Waveform design for active sensing systems: A computational approach*. Cambridge University Press, 2012.
- [41] R. W. Gerchberg and W. O. Saxton, "A practical algorithm for the determination of the phase from image and diffraction plane pictures," *Optik*, vol. 35, p. 237–246, 1972.
- [42] P. Jaming, "Uniqueness results in an extension of Pauli's phase retrieval problem," *Applied and Computational Harmonic Analysis*, vol. 37, no. 3, pp. 413–441, 2014.
- [43] L. B. Almeida, "The fractional Fourier transform and time-frequency representations," *IEEE Transactions on Signal Processing*, vol. 42, no. 11, pp. 3084–3091, 1994.
- [44] K. Jaganathan, Y. C. Eldar, and B. Hassibi, "STFT phase retrieval: Uniqueness guarantees and recovery algorithms," *IEEE Journal of Selected Topics in Signal Processing*, vol. 10, no. 4, pp. 770–781, 2016.
- [45] S. Nawab, T. Quatieri, and J. Lim, "Signal reconstruction from short-time Fourier transform magnitude," *IEEE Transactions on Acoustics, Speech, and Signal Processing*, vol. 31, no. 4, pp. 986–998, 1983.
- [46] Y. C. Eldar, P. Sidorenko, D. G. Mixon, S. Barel, and O. Cohen, "Sparse phase retrieval from short-time Fourier measurements," *IEEE Signal Processing Letters*, vol. 22, no. 5, pp. 638–642, 2014.
- [47] T. Bendory, Y. C. Eldar, and N. Boumal, "Non-convex phase retrieval from STFT measurements," *IEEE Transactions on Information Theory*, vol. 64, no. 1, pp. 467–484, 2018.
- [48] T. Bendory, P. Sidorenko, and Y. C. Eldar, "On the uniqueness of FROG methods," *IEEE Signal Processing Letters*, vol. 24, no. 5, pp. 722–726, 2017.
- [49] S. Pinilla, T. Bendory, Y. C. Eldar, and H. Arguello, "Frequency-resolved optical gating recovery via smoothing gradient," *IEEE Transactions on Signal Processing*, vol. 67, no. 23, pp. 6121–6132, 2019.
- [50] Y. Shechtman, Y. C. Eldar, O. Cohen, H. N. Chapman, J. Miao, and M. Segev, "Phase retrieval with application to optical imaging: A contemporary overview," *IEEE Signal Processing Magazine*, vol. 32, no. 3, pp. 87–109, 2015.
- [51] N. Vaswani, "Nonconvex structured phase retrieval: A focus on provably correct approaches," *IEEE Signal Processing Magazine*, vol. 37, no. 5, pp. 67–77, 2020.
- [52] J. Ranieri, A. Chebira, Y. M. Lu, and M. Vetterli, "Phase retrieval for sparse signals: Uniqueness conditions," *arXiv preprint arXiv:1308.3058*, 2013.
- [53] S. Pinilla, K. V. Mishra, B. M. Sadler, and H. Arguello, "BanRaW: Band-limited radar waveform design via phase retrieval," in *IEEE International Conference on Acoustics, Speech and Signal Processing*, 2021, pp. 5449–5453.
- [54] K. Jaganathan, J. Saunderson, M. Fazei, Y. C. Eldar, and B. Hassibi, "Phaseless super-resolution using masks," in *IEEE International Conference on Acoustics, Speech and Signal Processing*, 2016, pp. 4039–4043.
- [55] E. J. Candés, X. Li, and M. Soltanolkotabi, "Phase retrieval via Wirtinger flow: Theory and algorithms," *IEEE Transactions on Information Theory*, vol. 61, no. 4, pp. 1985–2007, 2015.
- [56] M. Hayes, "The reconstruction of a multidimensional sequence from the phase or magnitude of its Fourier transform," *IEEE Transactions on Acoustics, Speech, and Signal Processing*, vol. 30, no. 2, pp. 140–154, 1982.
- [57] T. Bendory, D. Edidin, and Y. C. Eldar, "Blind phaseless short-time Fourier transform recovery," *IEEE Transactions on Information Theory*, vol. 66, no. 5, pp. 3232–3241, 2019.
- [58] R. Beinert and G. Plonka, "Enforcing uniqueness in one-dimensional phase retrieval by additional signal information in time domain," *Applied and Computational Harmonic Analysis*, vol. 45, no. 3, pp. 505–525, 2018.
- [59] H. Zhang and Y. Liang, "Reshaped Wirtinger flow for solving quadratic system of equations," in *Advances in Neural Information Processing Systems*, vol. 29, 2016, pp. 2622–2630.
- [60] S. Pinilla, J. Bacca, and H. Arguello, "Phase retrieval algorithm via non-convex minimization using a smoothing function," *IEEE Transactions on Signal Processing*, vol. 66, no. 17, pp. 4574–4584, 2018.
- [61] J. Nocedal and S. Wright, *Numerical optimization*. Springer Science & Business Media, 2006.
- [62] R. Hunger, "An introduction to complex differentials and complex differentiability," Technische Universität München, Tech. Rep. TUM-LNS-TR-07-06, 2007.
- [63] J. C. Spall, *Introduction to stochastic search and optimization: Estimation, simulation, and control*, ser. Wiley-Interscience Series in Discrete Mathematics and Optimization. John Wiley & Sons, 2005.
- [64] N. Parikh and S. Boyd, "Proximal algorithms," *Foundations and Trends in optimization*, vol. 1, no. 3, pp. 127–239, 2014.

- [65] S. Ghadimi and G. Lan, “Stochastic first-and zeroth-order methods for nonconvex stochastic programming,” *SIAM Journal on Optimization*, vol. 23, no. 4, pp. 2341–2368, 2013.
- [66] W. Rudin, *Functional Analysis*, 2nd ed. McGraw-Hill, 1991.
- [67] C. Zhang and X. Chen, “Smoothing projected gradient method and its application to stochastic linear complementarity problems,” *SIAM Journal on Optimization*, vol. 20, no. 2, pp. 627–649, 2009.
- [68] J. C. Duchi and F. Ruan, “Solving (most) of a set of quadratic equalities: Composite optimization for robust phase retrieval,” *Information and Inference: A Journal of the IMA*, vol. 8, no. 3, pp. 471–529, 2019.